Synthesis and Application of Fluorescent Tryptanthrin Derivatives

（*Sep. 17, 2017 at Iwate University*）

Jun Kawakami
Graduate School of Science and Technology,
Hirosaki University

Tryptanthrin

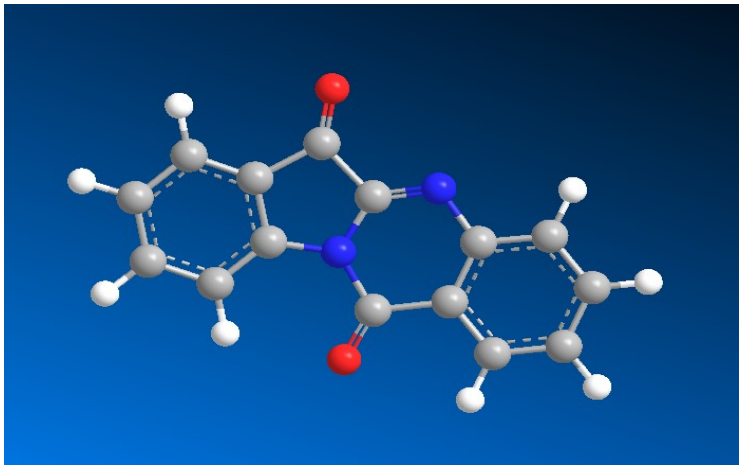

スキンケア用途に適した新規タデ藍エキス
弘前大学とサンスター株式会社が共同開発

2013年4月22日
国立大学法人弘前大学
サンスター株式会社

国立大学法人弘前大学（青森県弘前市、以下：弘前大学）とサンスター株式会社（本社：大阪府高槻市、代表取締役社長 吉岡貴司、以下：サンスター）は、2007年8月に締結した「研究連携の推進に係る協定」に基づき、2009年6月よりタデ藍の抗真菌活性に着目した共同研究に取り組み、このたび、新規タデ藍エキスを開発、スキンケア用途での有用性を使用試験により確認しました。

○タデ藍抽出物「トリプタンスリン」に抗真菌活性
↓
○新規タデ藍エキスの開発
↓
○新規タデ藍エキスの有用性確認

研究の背景

タデ藍（Polygonum tinctrium (ポリゴナムチンクトリウム)）は、日本における藍染め染料の原料植物としてよく知られていますが、古くから様々な薬効が言い伝えられた民間伝承薬としても用いられました。近年、弘前大学教育学部北原晴男教授を中心とし、染色以外の可能性として、抗真菌性に注目した研究が始まりました。北原晴男教授らは、タデ藍から高い抗真菌性を示す物質「トリプタンスリン」を単離し、これらの研究成果を基に、タデ藍の持つ抗真菌活性を応用した外用剤等の開発を目指して、弘前大学とサンスター株式会社は共同研究を実施しました。

＜タデ藍の畑＞　＜タデ藍＞　＜新規タデ藍エキス＞

http://jp.sunstar.com/company/press/2013/0422.html

Qiana -キアナ-

「Qiana（キアナ）」は、サンスターが女性のために開発した、不安定肌を健やかに保つためのスキンケアブランドです。

「くり返す不安定肌」に。

いつもと同じお手入れをしているのに、肌の調子がよい時と悪い時がある…。
昨日までなかった突然の肌あれが一日中気になってしまう。

サンスターは、そんなくり返される大人の女性の肌なやみを研究。
植物に宿る天然の手力に着目し、サンスター独自の方法で抽出した
"藍潤エキス"を配合。

独自の方法で抽出し、高濃度エキス化した
"藍潤エキス※"を配合

古くから、多くの有用性が伝えられている"藍"の、肌に対する働きに着目。

香川の特定農場で丹精に育てた"藍"を独自の抽出法により高濃度エキス化、全アイテムに配合。

女性のくり返される不安定肌を、健やかに保ちます。

藍潤エキス
トリプタンスリンなど、お肌を健やかに保つ成分が含まれている藍を、サンスター独自の抽出法で高濃度エキス化。

保湿成分

ヨモギ葉エキス
ヨモギにはフラボノイドやタンニン、多糖類などお肌を健やかに保つ成分が含まれています。

ヒアルロン酸
水分を抱く力が高く、皮膚にうるおいを与えるのに重要な成分。皮膚にとどまり、角質層に水分をとどめます。

※ 藍潤エキス(保湿成分)とは、アイ葉／藍エキスのことです。

http://jp.sunstar.com/products/brand/qiana/

Tryptanthrin is a weakly basic alkaloid found in a number of plant specie. It demonstrates a significant antifungal activity against *Malassezia furfur*, which causes atopic dermatitis, and is also effective in the treatment of contact dermatitis (delayed-type allergy).

H. Kitahara, K. Hanada, T. Fukui, Antimicrobial active agents from the Japanese indigo plant and the various compositions of them, Patent No. 5239002, Japan, (Apr. 12, 2013).
H. Kitahara, Y. Sato, D. Ishikawa, K. Kumazawa, A. Nakane, and K. Hanada, Type IV allergic reaction inhibitor, Patent No. 5023317, Japan, (Jun. 29, 2012).

Synthesis of tryptanthtin derivatives

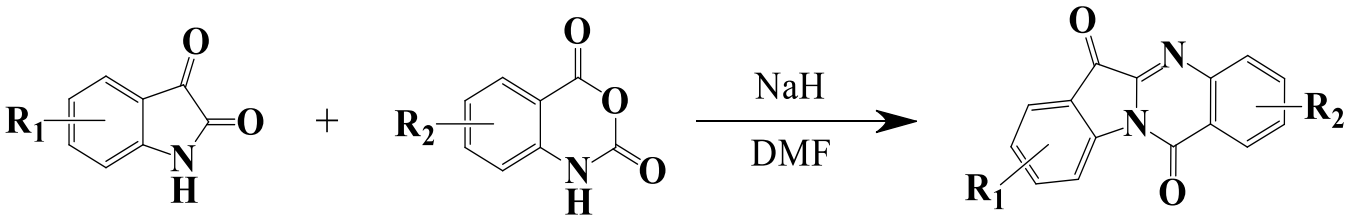

isatin derivatives isatoic anhydride derivatives tryptanthtin derivatives

L. A. Mitscher *et al., Heterocycles*, **1981**, *15*, 1017-1021.

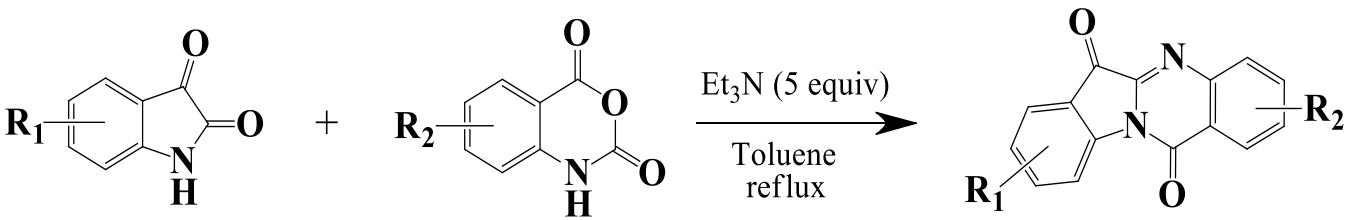

isatin derivatives isatoic anhydride derivatives tryptanthtin derivatives

V. M. Sharma *et al*., *Bioorganic & Medicinal Chemistry Letters*, **2002**, *12*, 2303–2307.

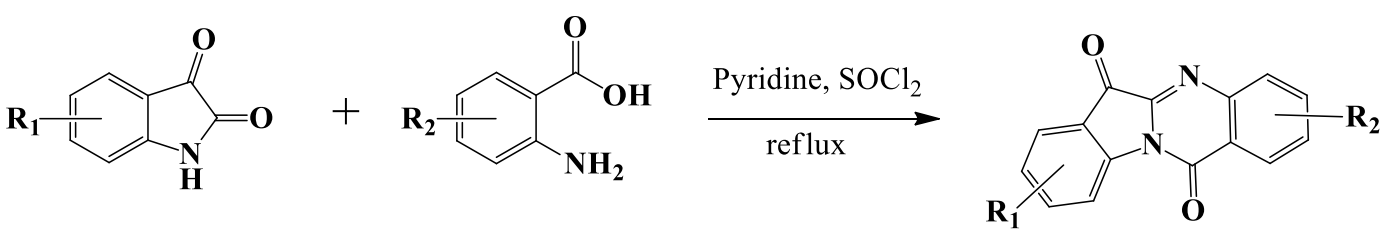

isatin derivatives anthranilic acid derivatives tryptanthtin derivatives

J. L. Liang et al., *Bioorganic & Medicinal Chemistry*, **2012**, *20*, 4962–4967.

Synthesis of isatin derivatives

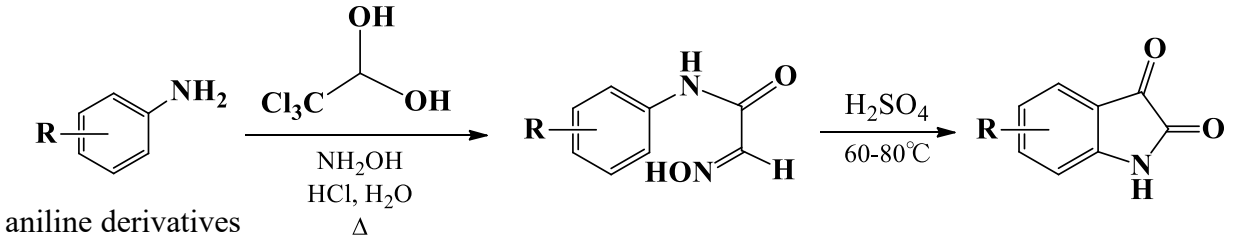

Organic Syntheses, **1941**, *Coll. Vol. 1*, p.327; **1925**, *Vol. 5*, p.71.

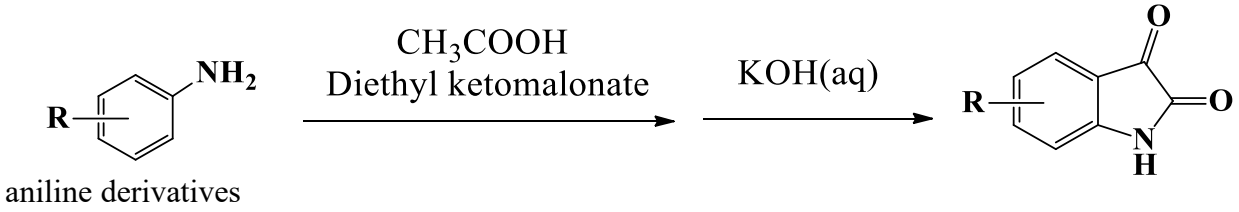

K. C. Rice *et al*., *J. Med. Chem*., **1976**, *19*, 887-892.

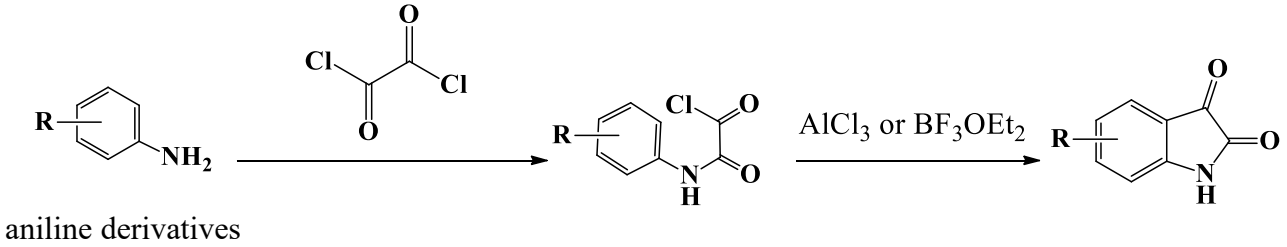

N. Kaila *et al*., J. *Med. Chem*., **2007**, *50*, 40-64.

Synthesis of isatoic anhydride derivatives

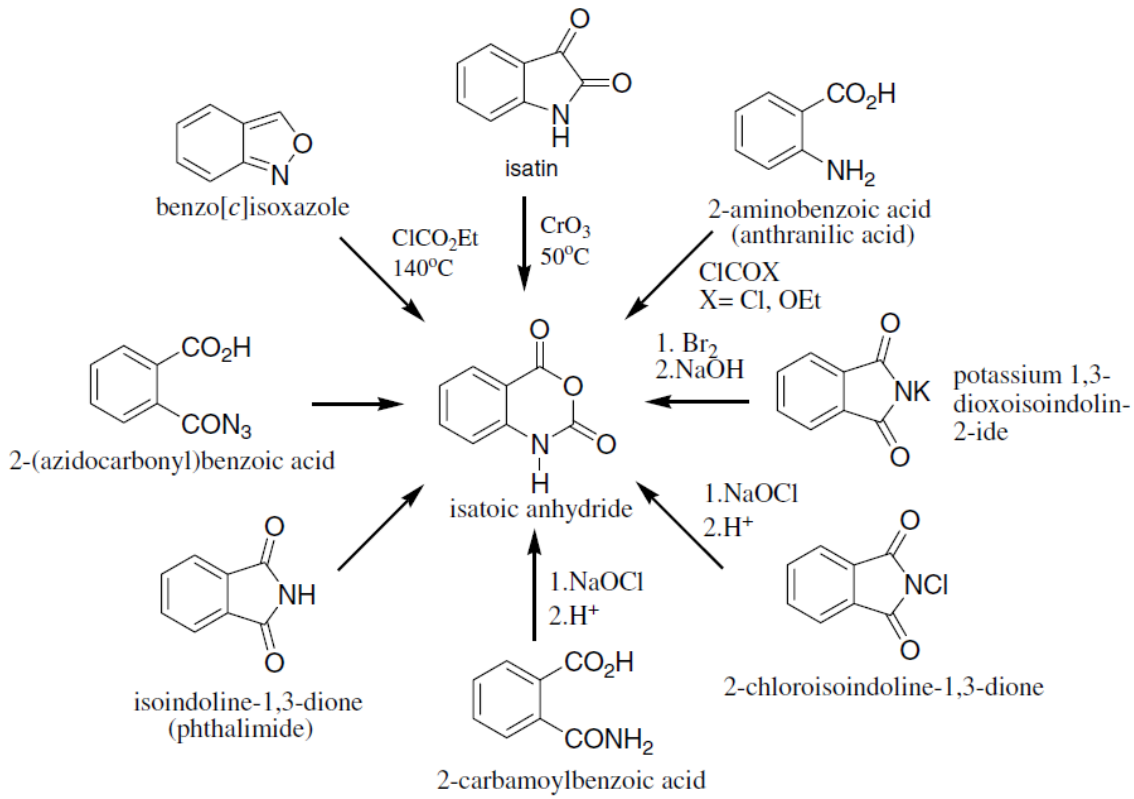

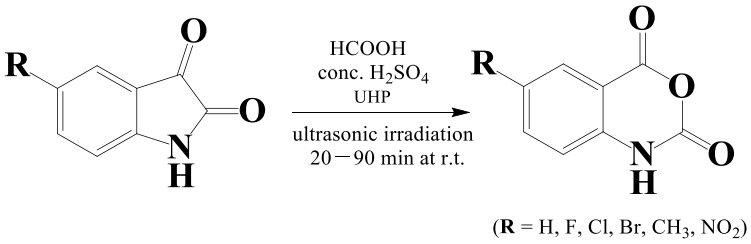

67－98%

T. Deligeorgiev, A. Vasilev, J. J. Vaquero, J. Alvarez-Builla, *Ultrasonics Sonochemistry*, **2007**, *14*, 497-501.

Antibacterial activity

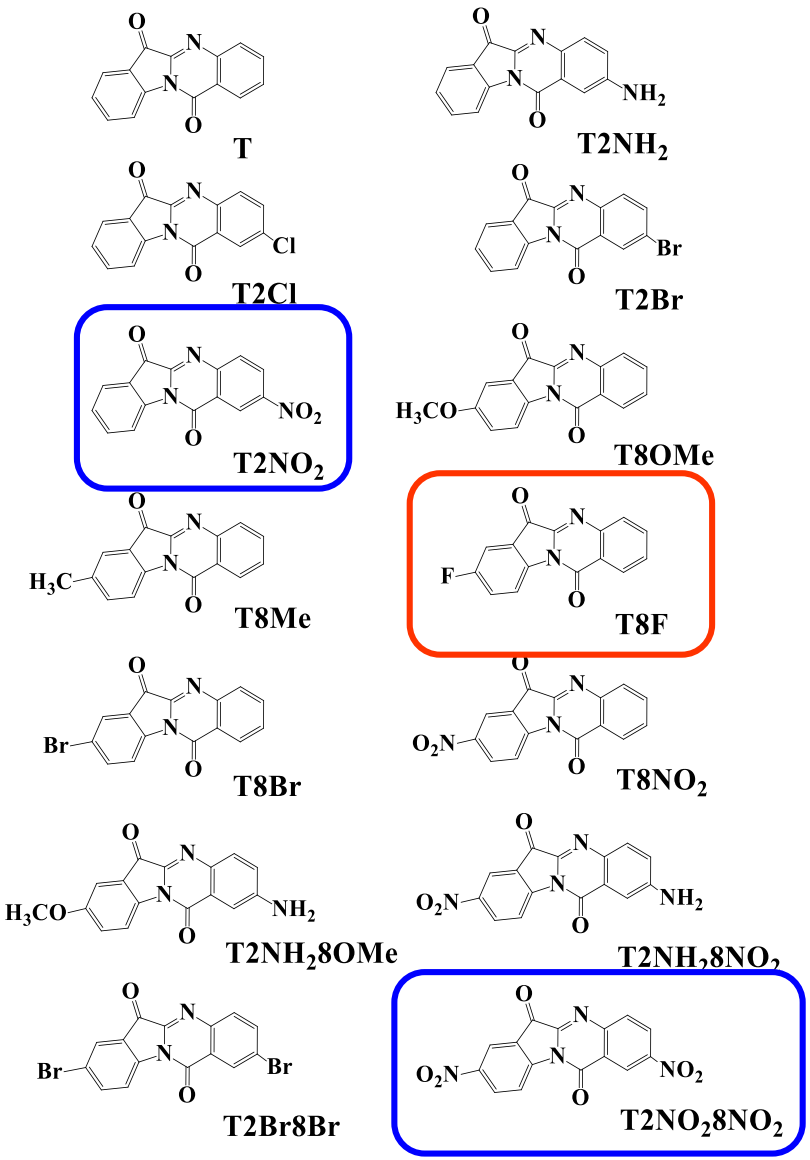

Antibacterial activity (MIC) of tryptanthrin (**T**) and its 13 derivatives against MRSA and *M. furfur*.

	MIC/μg mL^{-1}	
	MRSA	*M. furfur*
T	0.5	4
T2NH$_2$	2.0	20
T2Cl	0.1	4
T2Br	0.3	4
T2NO$_2$	>100	>160
T8OMe	2.5	>120
T8Me	0.5	>120
T8F	0.1	1
T8Br	0.1	2.5
T8NO$_2$	0.5	4
T2NH$_2$8OMe	2.0	20
T2NH$_2$8NO$_2$	0.5	>160
T2Br8Br	0.6	4
T2NO$_2$8NO$_2$	>100	>160

MIC = minimum inhibitory concentration in mg/mL.

J. Kawakami, N. Matsushima, Y. Ogawa, H. Kakinami, A. Nakane, H. Kitahara, M. Nagaki, and S. Ito, *Trans. Mater. Res. Soc. Japan*, **2011**, *36*, 603-606.

Corrilation of MIC with LUMO

	MIC/μg mL^{-1}	
	MRSA	*M. furfur*
T	0.5	4
T8F	0.1	1
T2NO$_2$	>100	>160

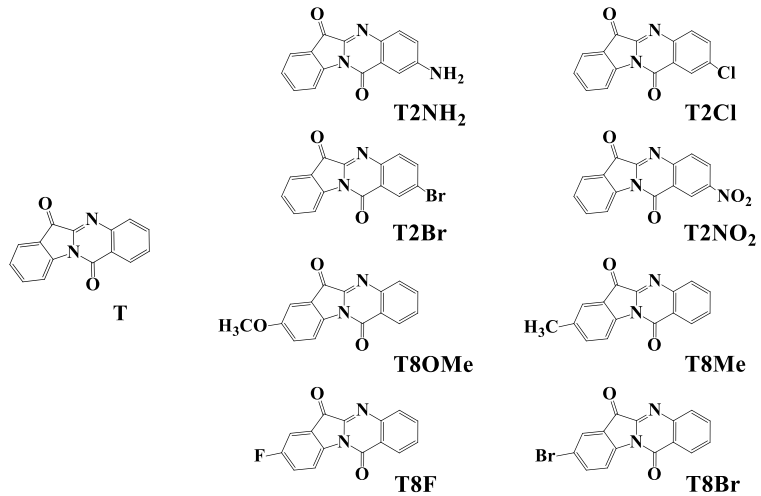

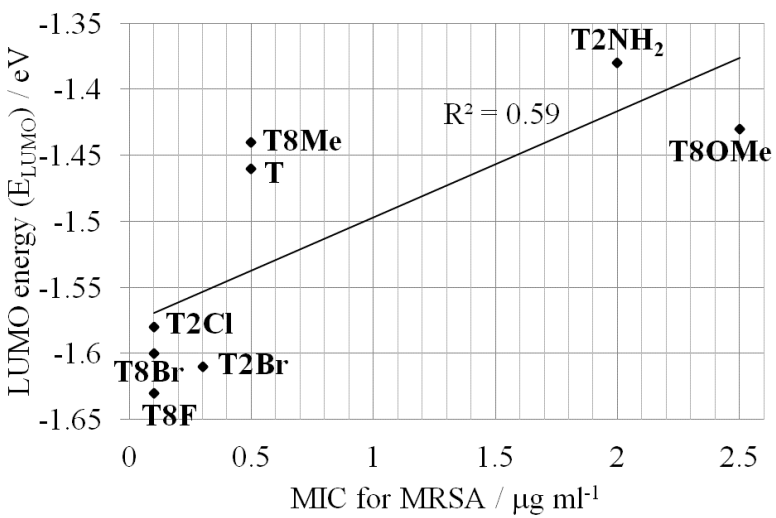

The lowest unoccupied molecular orbital (LUMO) energy against the antibacterial activity of tryptanthrin (R^2 = 0.59)[4].

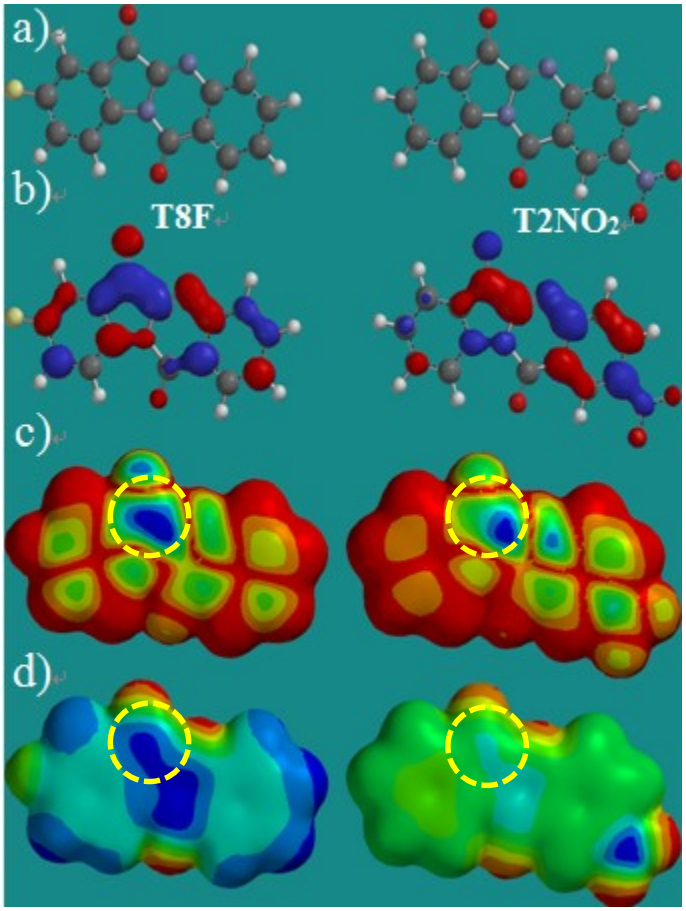

Molecular properties of **T8F** and **T2NO$_2$** by semi-empirical molecular orbital calculations (PM3); a) Molecular structures, b) molecular orbital of LUMO, c) LUMO maps and d) electrostatic potential maps.

J. Kawakami, H. Kakinami, N. Matsushima, A. Nakane, H. Kitahara, M. Nagaki, and S. Ito, *J. Comput. Chem. Jpn.*, **2013**, *12*, 109-112.

Triptanthrin and its derivatives

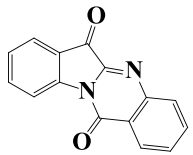

T
(Tryptanthrin)

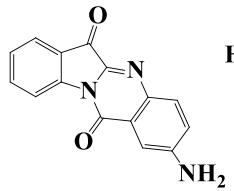

T2NH$_2$

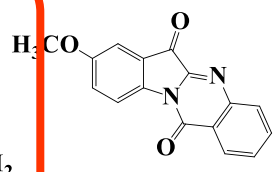

T8OMe

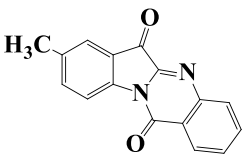

T8Me

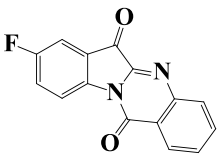

T8F

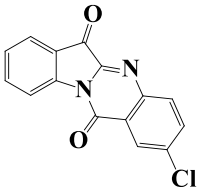

T2Cl

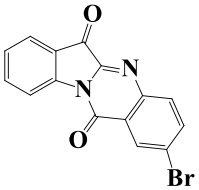

T2Br

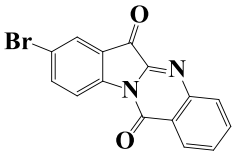

T8Br

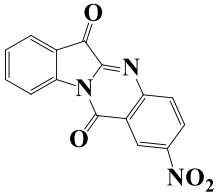

T2NO$_2$

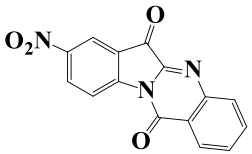

T8NO$_2$

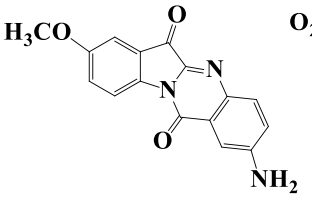

T2NH$_2$8OMe

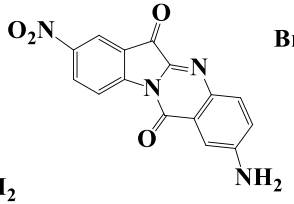

T2NH$_2$8NO$_2$

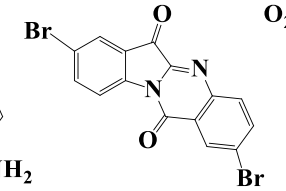

T2Br8Br

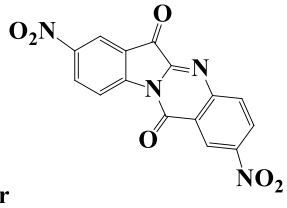

T2NO$_2$8NO$_2$

Absorption spectra of tryptanthrin derivatives

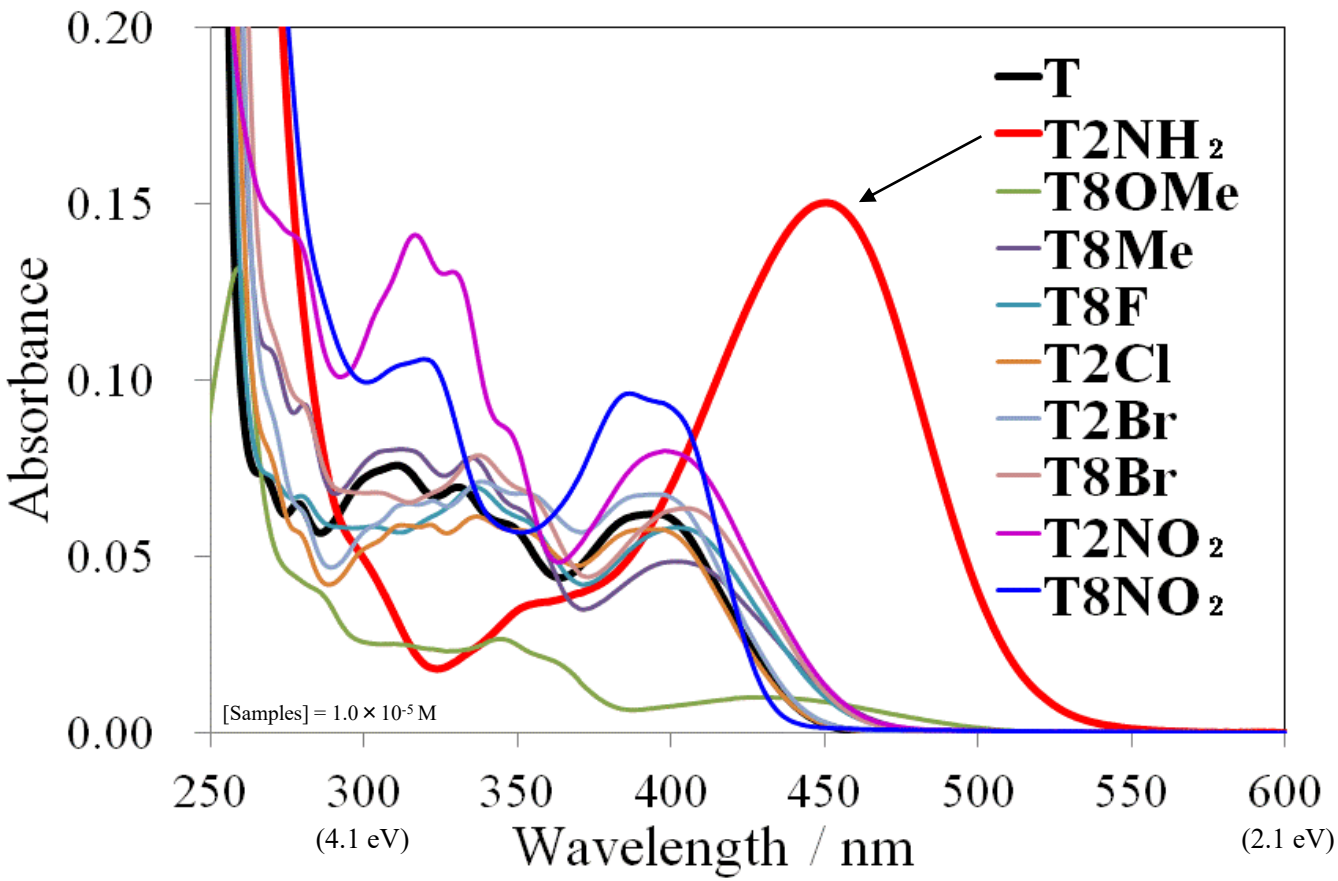

Absorption spectra of **T** and its nine derivatives in MeCN.

Fluorescence spectra tryptanthrin derivatives

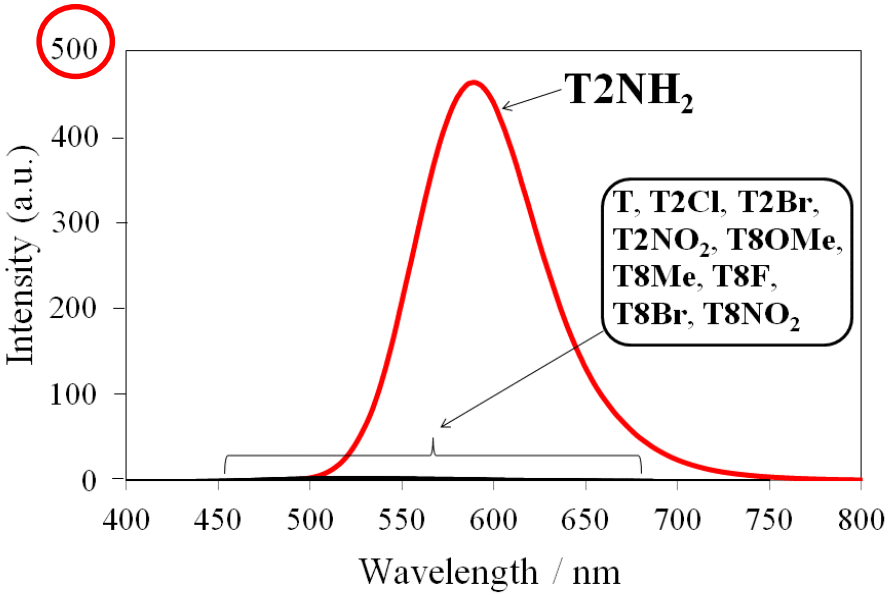

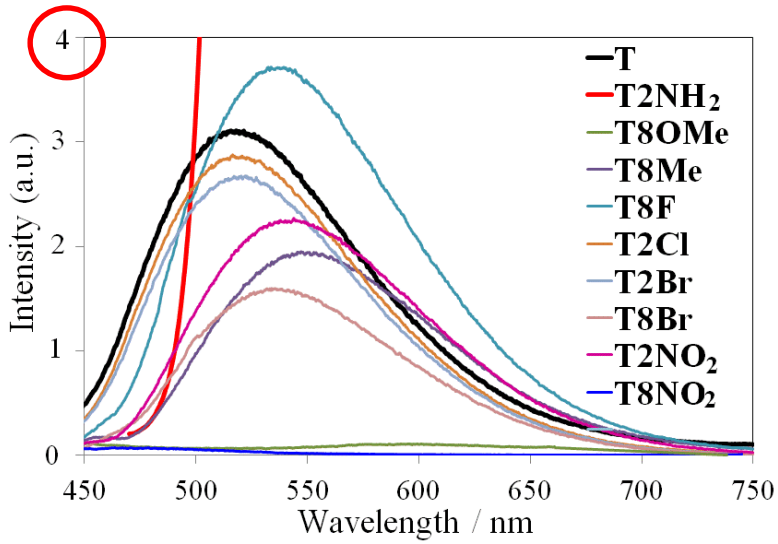

Fluorescence spectra of **T** and its nine derivatives in MeCN.

Absorption spectra of $T2NH_2$

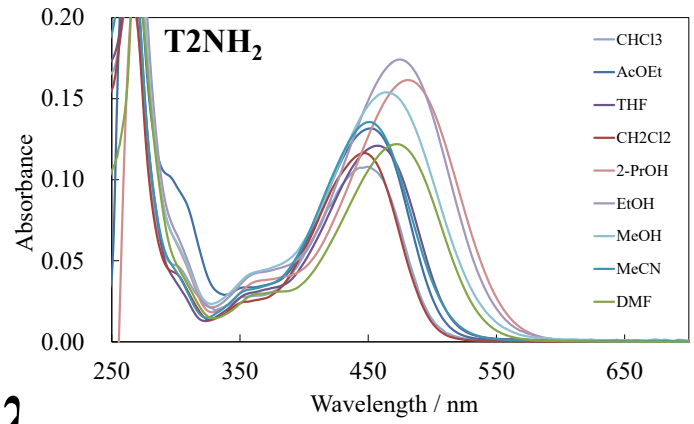

ε vs $\lambda_{a,\,max}$

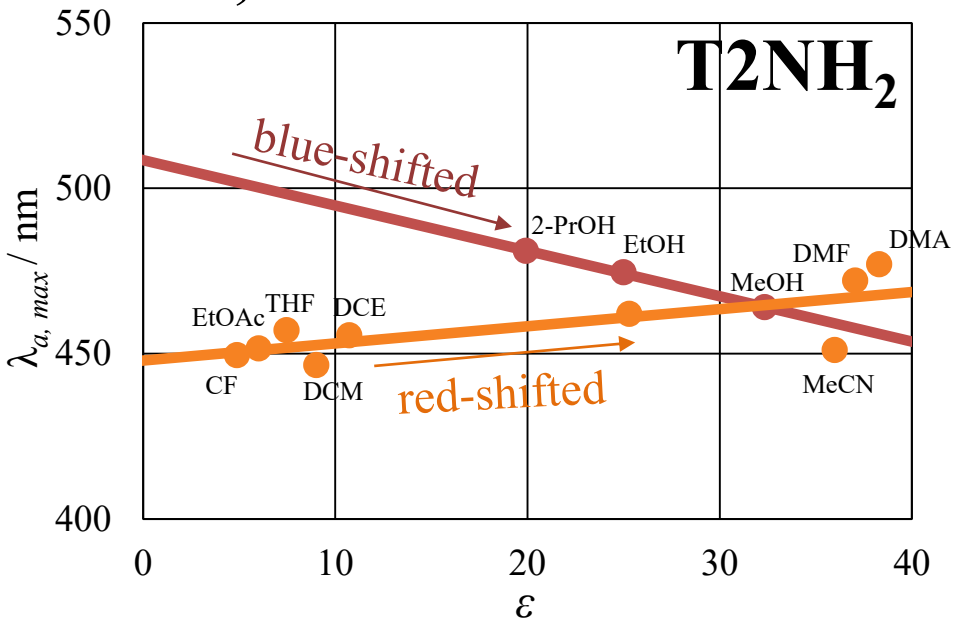

● : protic solvents

● : aprotic solvents

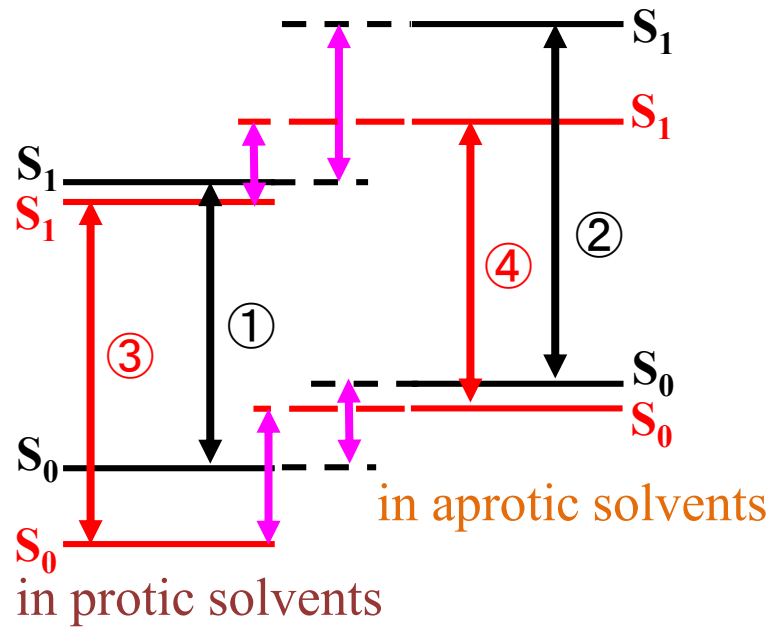

↕ : Stabilization by hydrogen bonding

—— : in low polar solvents

—— : in highly polar solvents

①＜②

①＜③

④＜②

③≒④

Fluorescent solvatochromism of 2-aminotryptanthrin

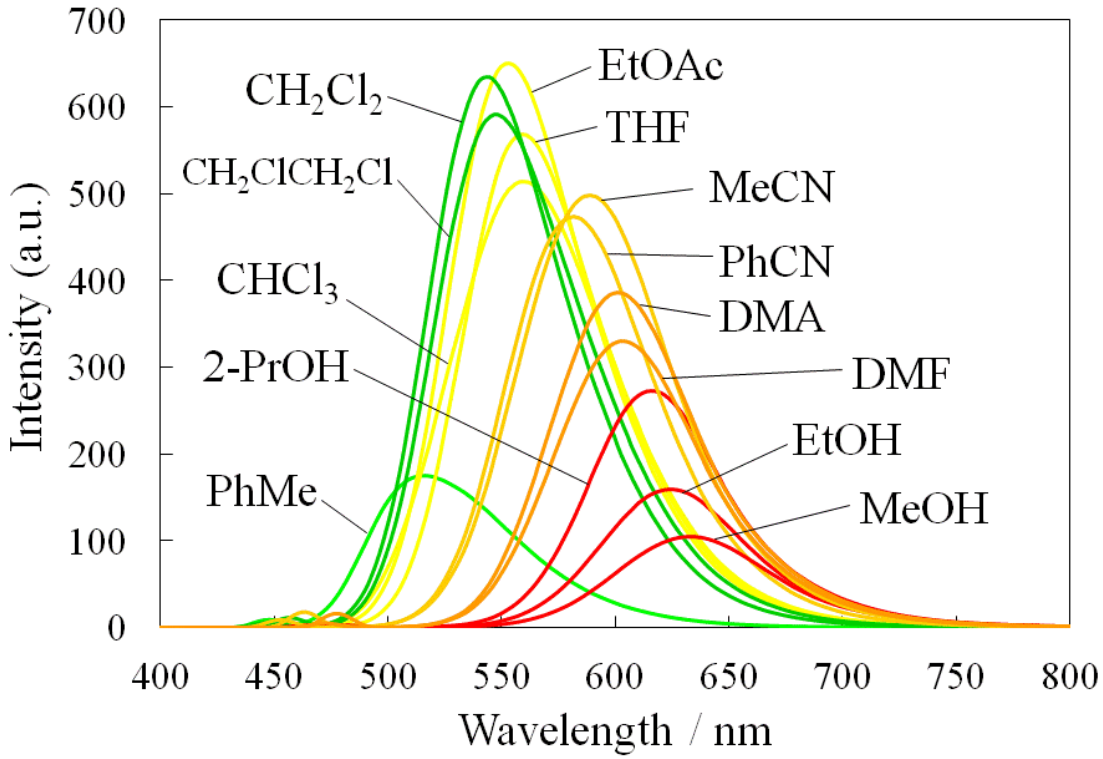

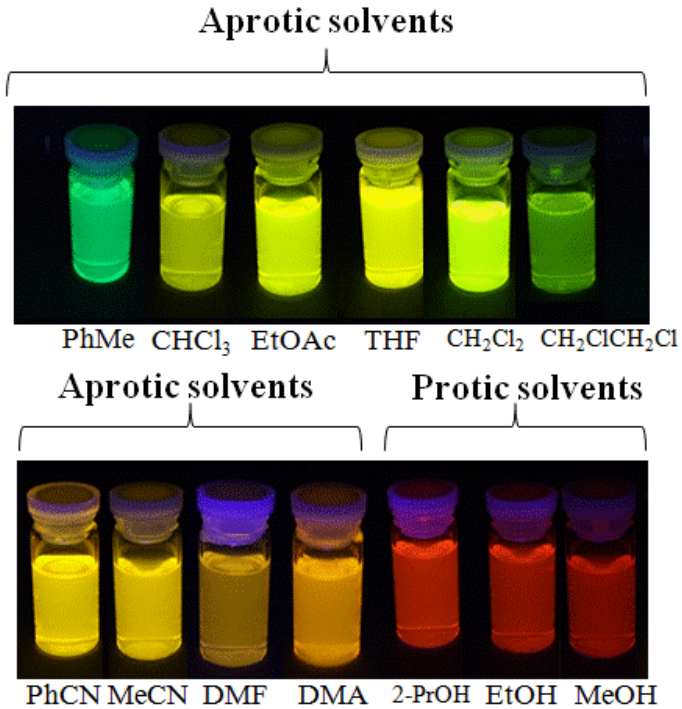

Florescence spectra in solvents of different polarity and photographs taken under UV light at 365 nm of **T2NH$_2$**.

J. Kawakami, Tryptanthrin Derivatives, Patent No. 5448046, Japan, (Jan. 10, 2014).

J. Kawakami, H. Kawaguchi, K. Kikuchi, A. Yamaya, S. Ito and H. Kitahara, *Trans. Mater. Res. Soc. Japan*, **2013**, *38*, 123-125.

ε vs $\lambda_{f,\,max}$

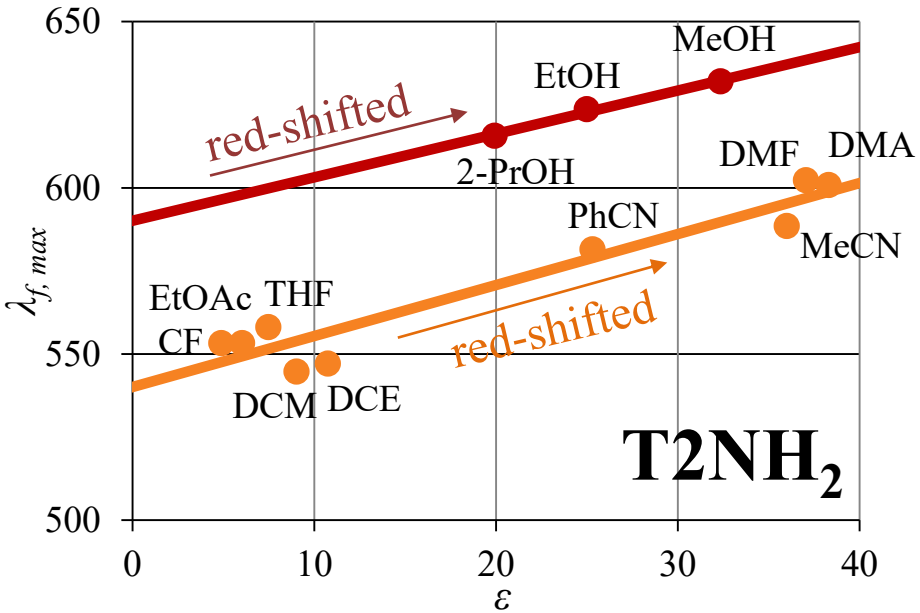

● : protic solvents

● : aprotic solvents

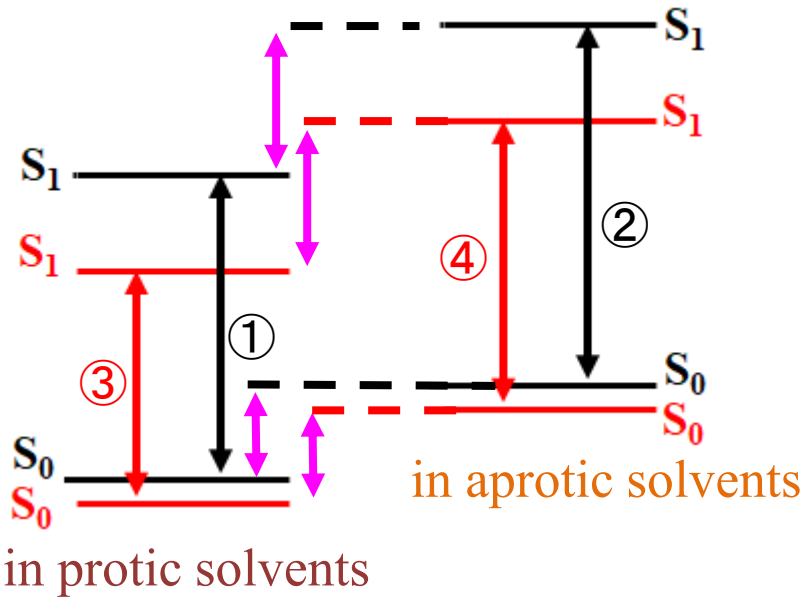

↕ : Stabilization by hydrogen bonding

—— : in low polar solvents

—— : in highly polar solvents

①＜②

①＞③

④＜②

③＜④

Intramolecular charge transfer (ICT) of T2NH$_2$

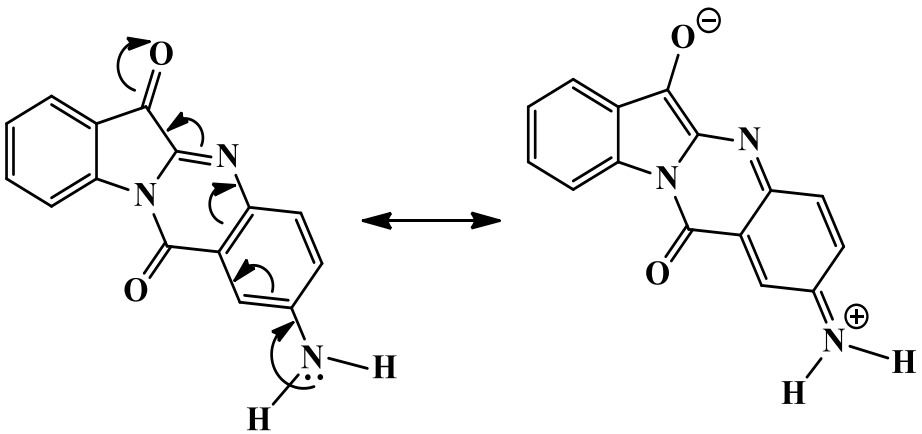

T2NH$_2$ possesses a planar polar structure with an effective intramolecular charge transfer (ICT) between the carbonyl group of the five-membered ring and the amino group.

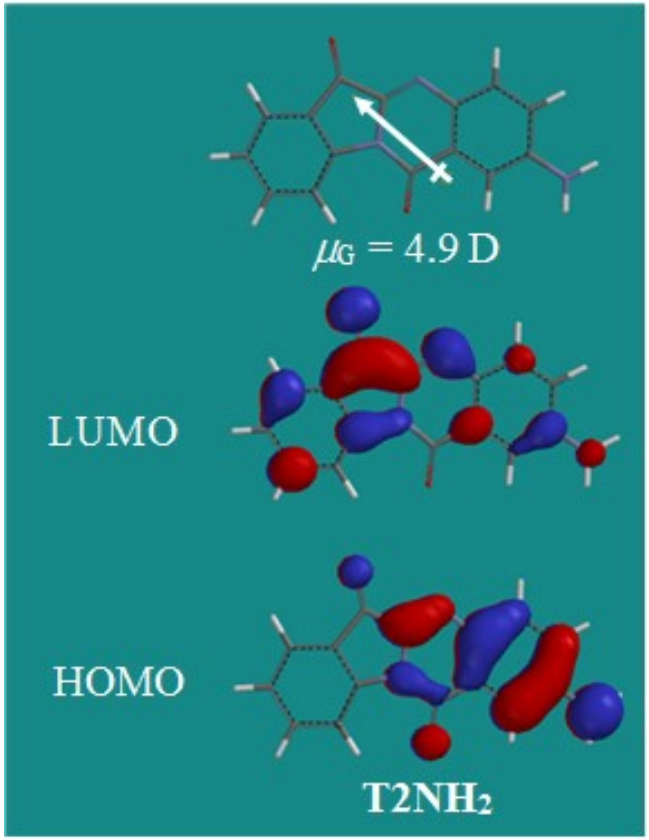

HOMO and LUMO surfaces and μ_G values of **T2NH$_2$** according to DFT calculations.

T

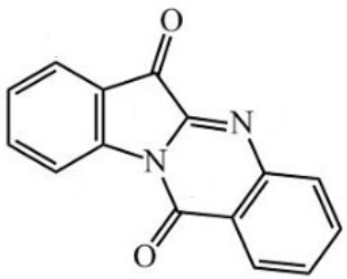

Tryptanthrin

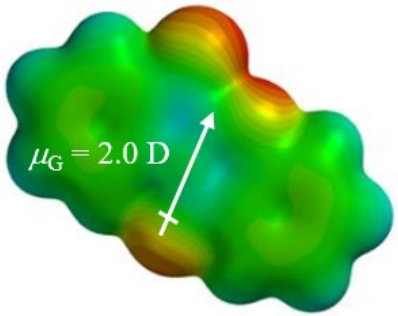

Electrostatic Potential Map

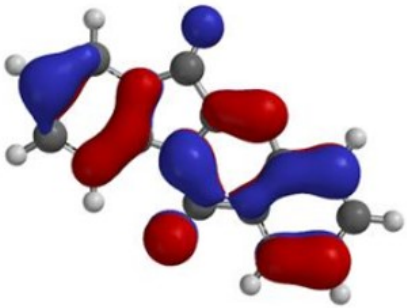

HOMO

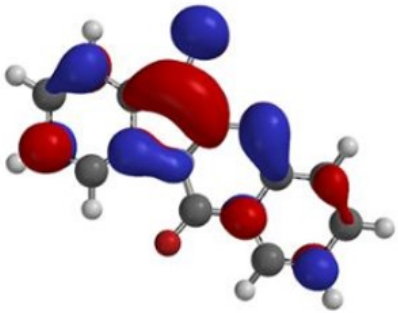

LUMO

T2NH$_2$

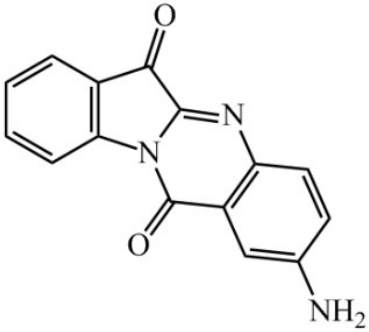

2-Aminotryptanthrin

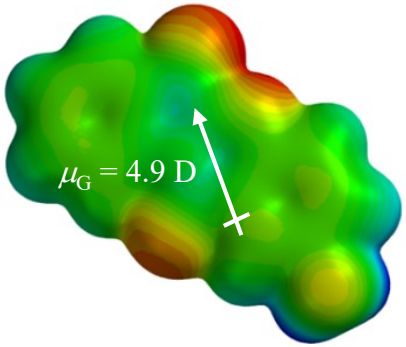

Electrostatic Potential Map

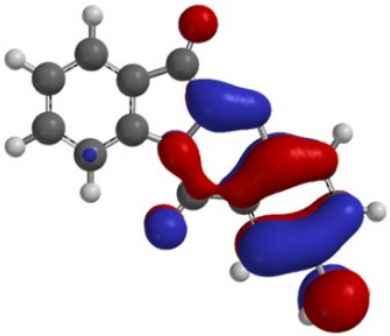

HOMO

LUMO

2-Aminotryptanthrin derivative with pyrene as a FRET-based fluorescent chemosensor for metal ions

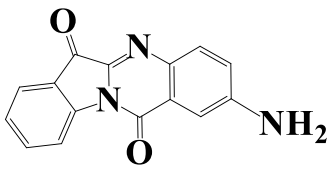

T2NH$_2$

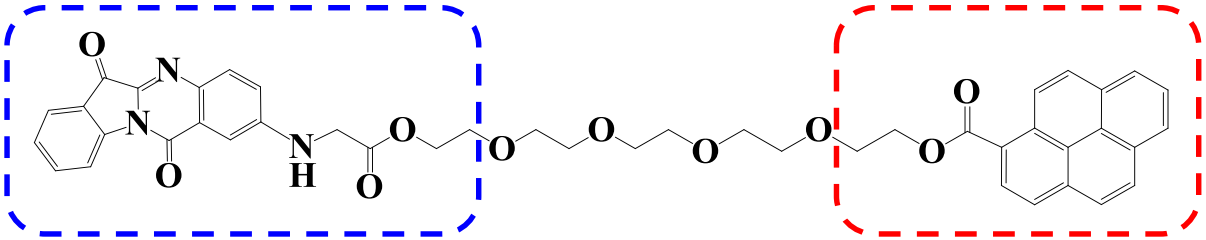

Energy acceptor（**A**）

T2NH-P5P

Energy donor（**D**）

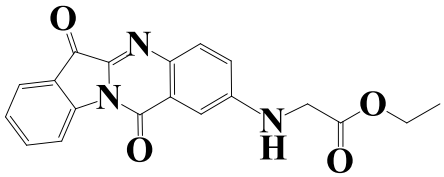

T2NH-CH$_2$COOEt

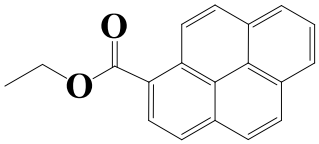

1EP

Structural formulae of **T2NH$_2$**, **T2NH-P5P**, **T2NH-CH$_2$COOEt**, and **1EP**.

Synthesis of T2NH-P5P

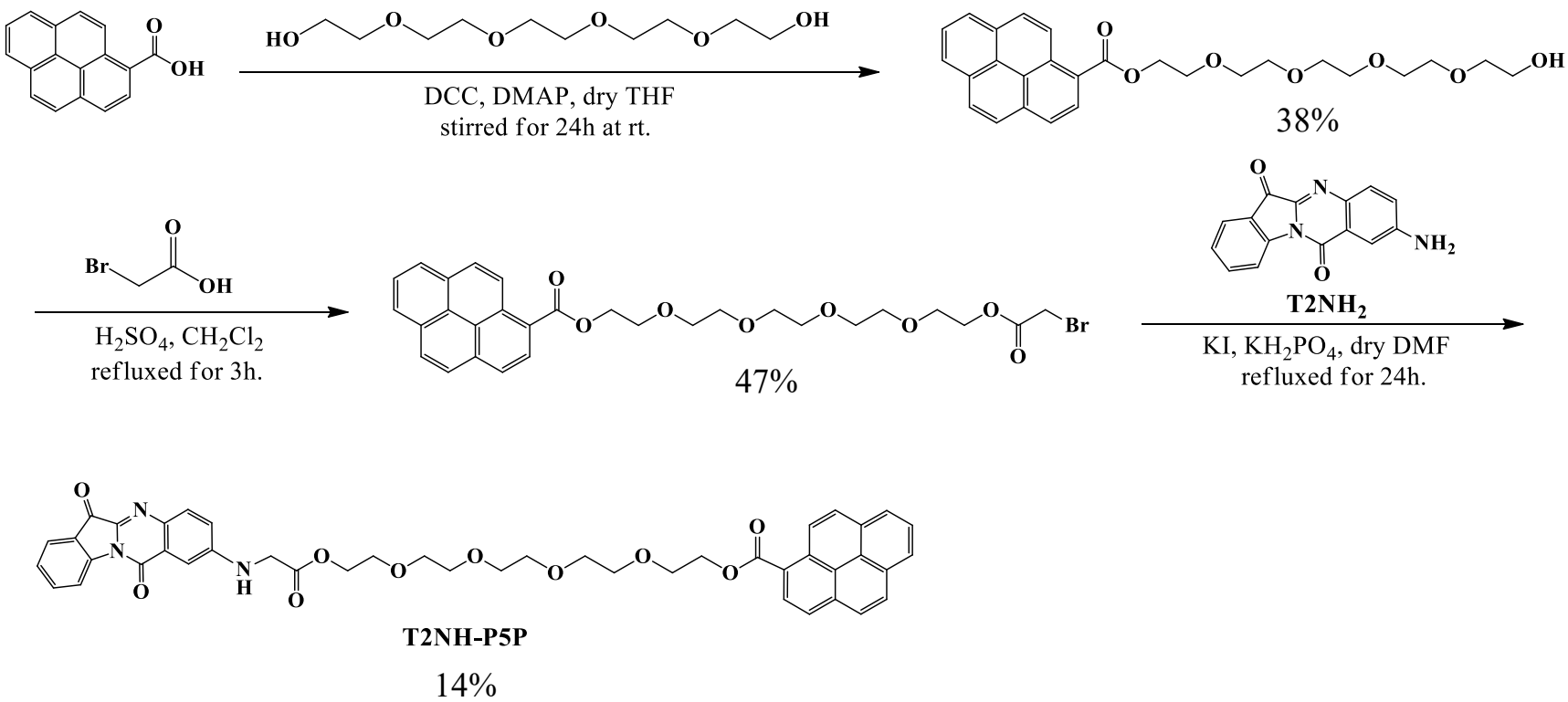

Fluorescence resonance energy transfer (FRET)

FEET is a mechanism describing energy transfer between two chromophores. A energy donor chromophore (**D**), initially in its electronic excited state, may transfer energy to an energy acceptor chromophore (**A**) through nonradiative dipole–dipole coupling. The efficiency of this energy transfer is inversely proportional to the sixth power of the distance between donor and acceptor, making FRET extremely sensitive to small changes in distance.

FRET-off

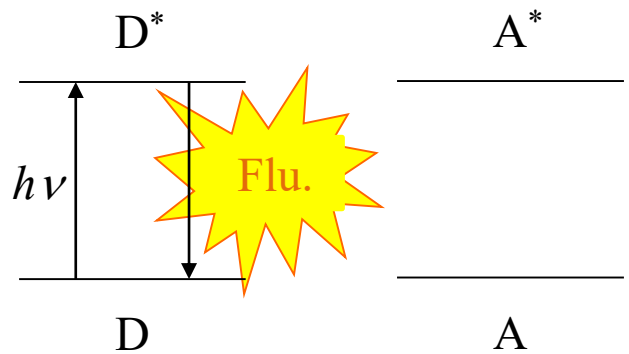

FRET-on

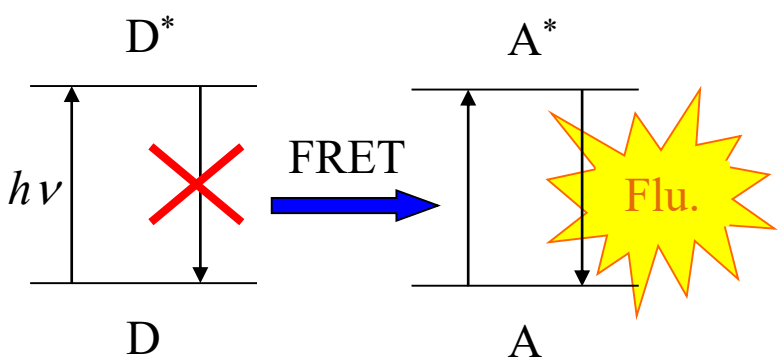

Requirements for FRET

- Suitable orientation of **D** and **A**.
- Suitable distance between **D** and **A**. (1－10 nm)
- Spectral overlap between the emission spectrum of **D** and the absorption spectrum of **A**.

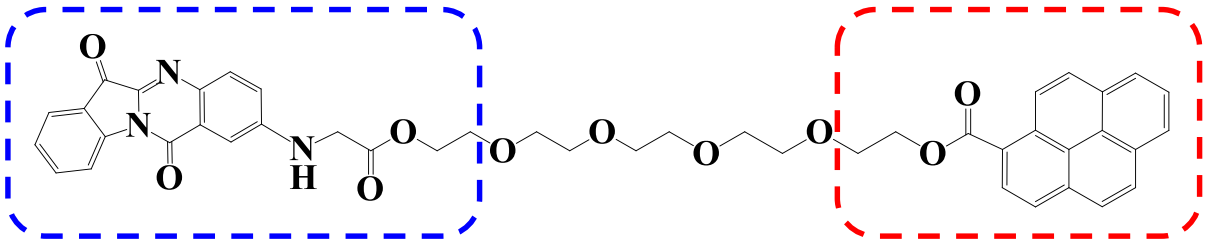

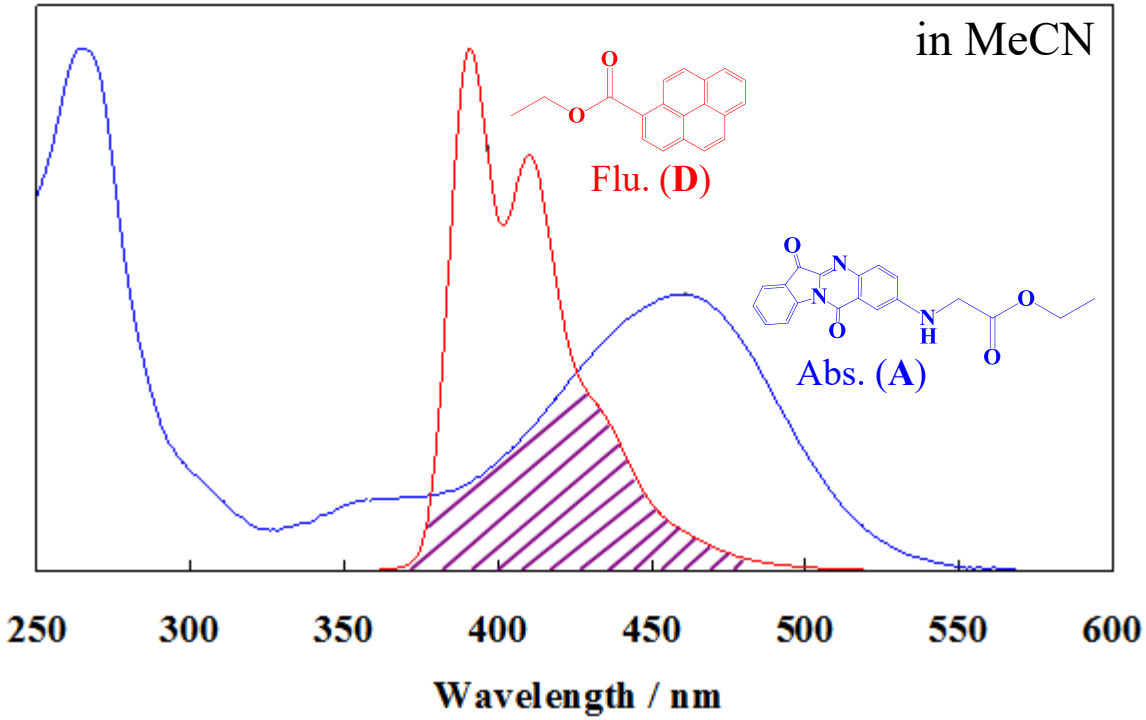

Spectral overlap between the emission spectrum of **D** and the absorption spectrum of **A**.

Absorption spectra

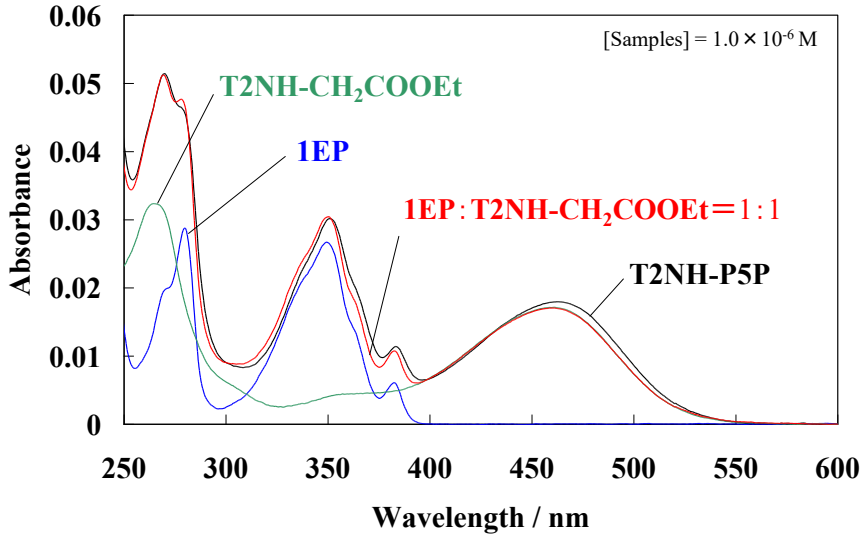

UV–vis absorption spectra of **T2NH-P5P** and an equimolar mixture of **T2NH-CH_2COOEt** and **1EP**, both in acetonitrile at room temperature.

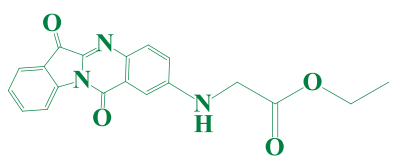

T2NH-CH_2COOEt

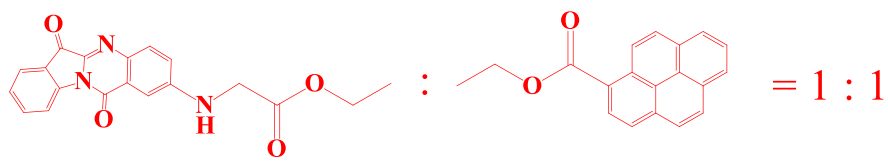

T2NH-CH_2COOEt **1EP**

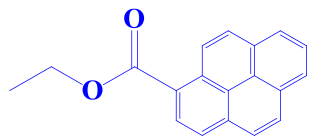

1EP

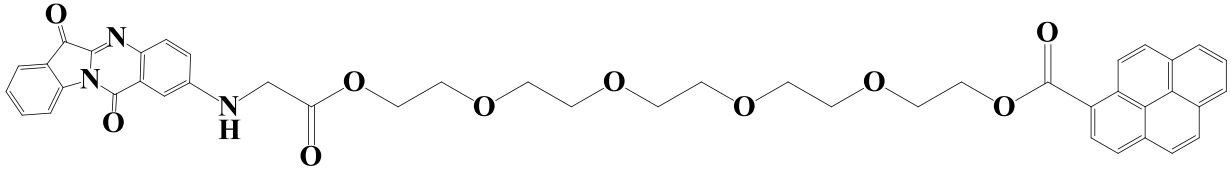

T2NH-P5P

Fluorescence spectra

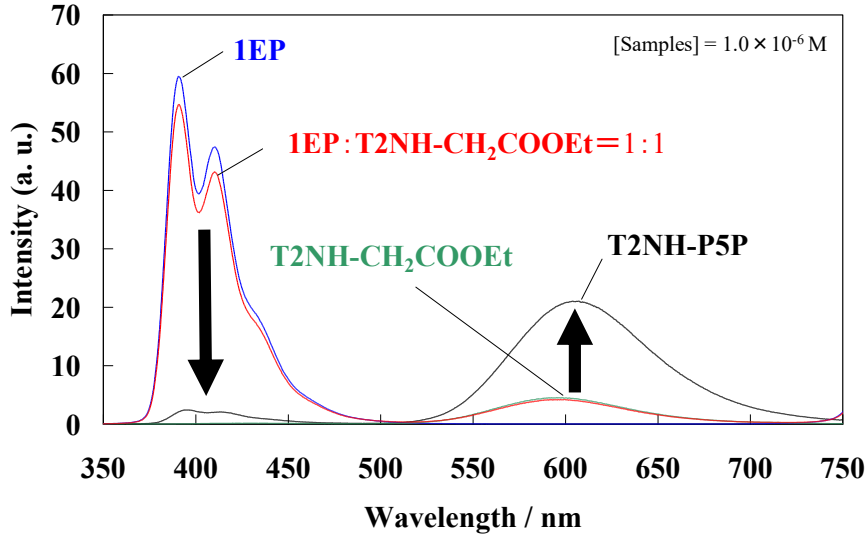

Fluorescence spectra of **T2NH-P5P** and an equimolar mixture of **T2NH-CH$_2$COOEt** and **1EP**, both excited at 325 nm in acetonitrile at room temperature.

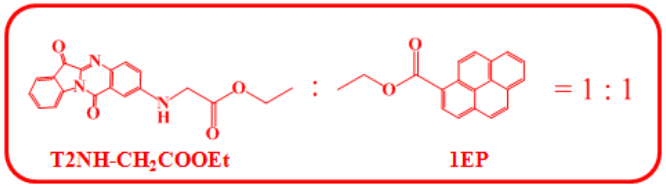

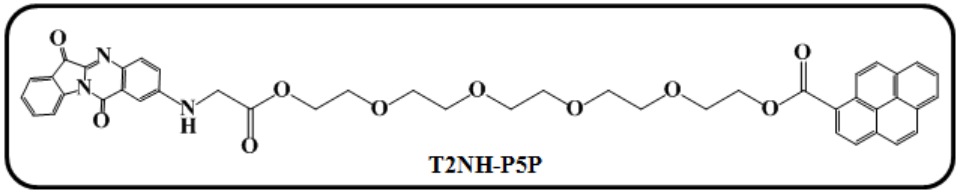

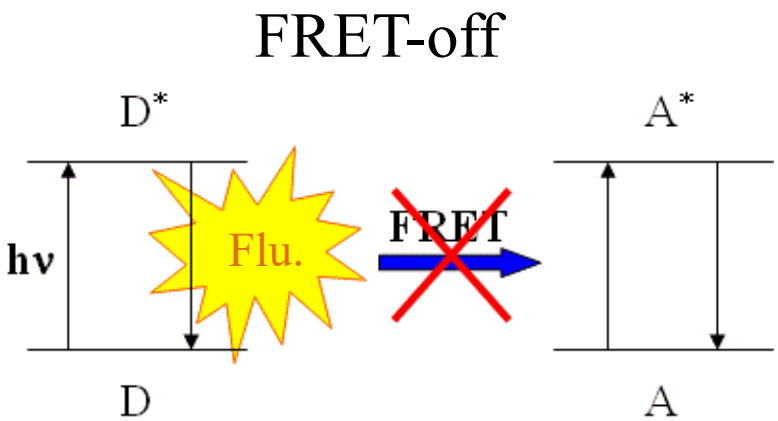

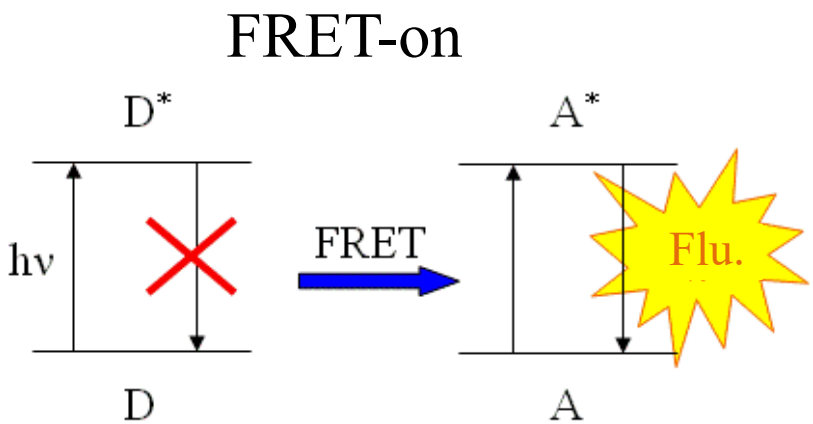

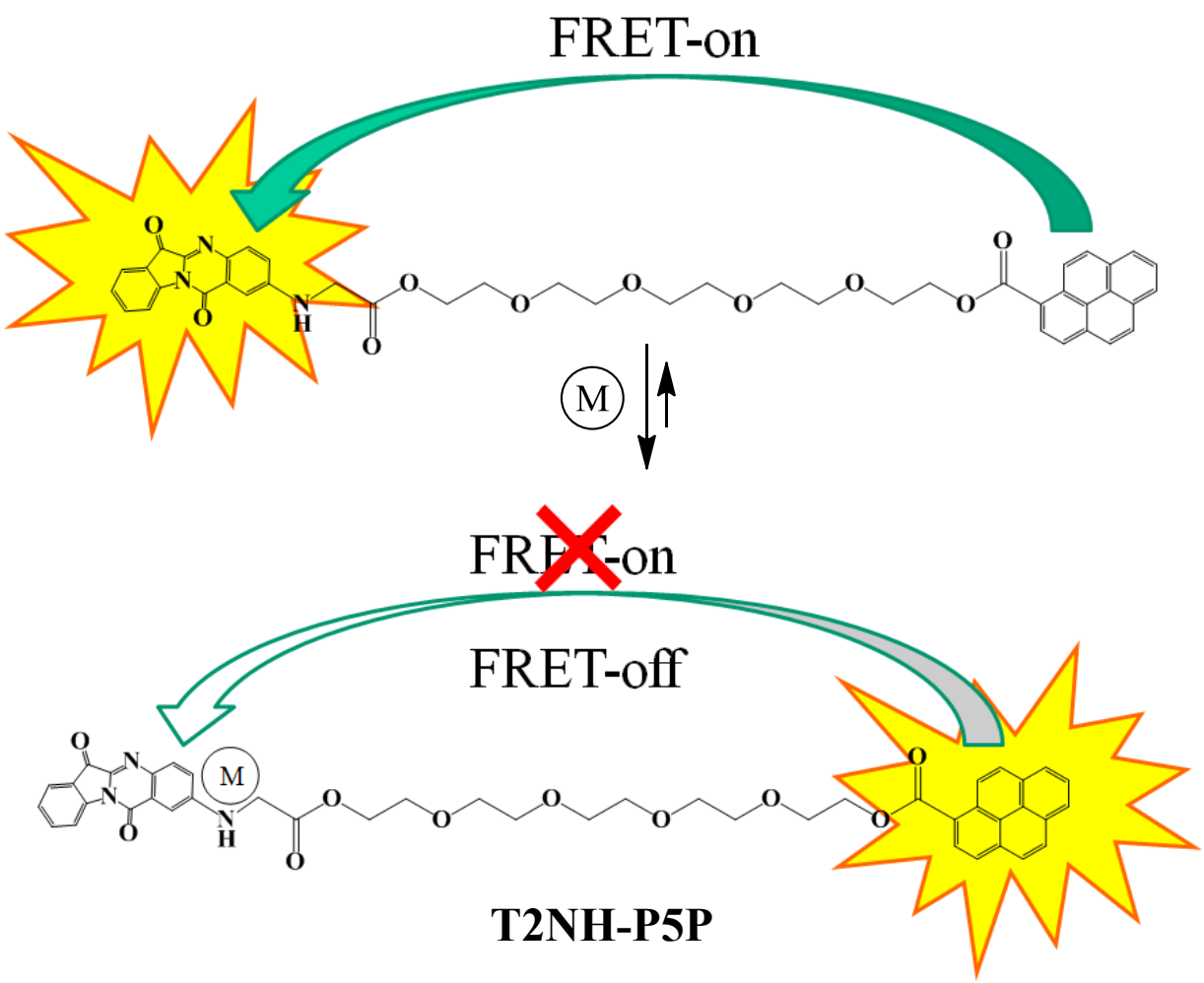

If the on-off of FRET is controlled by certain metal ions, **T2NH-P5P** can be used as a FRET-type fluorescent chemosensor for metal ions.

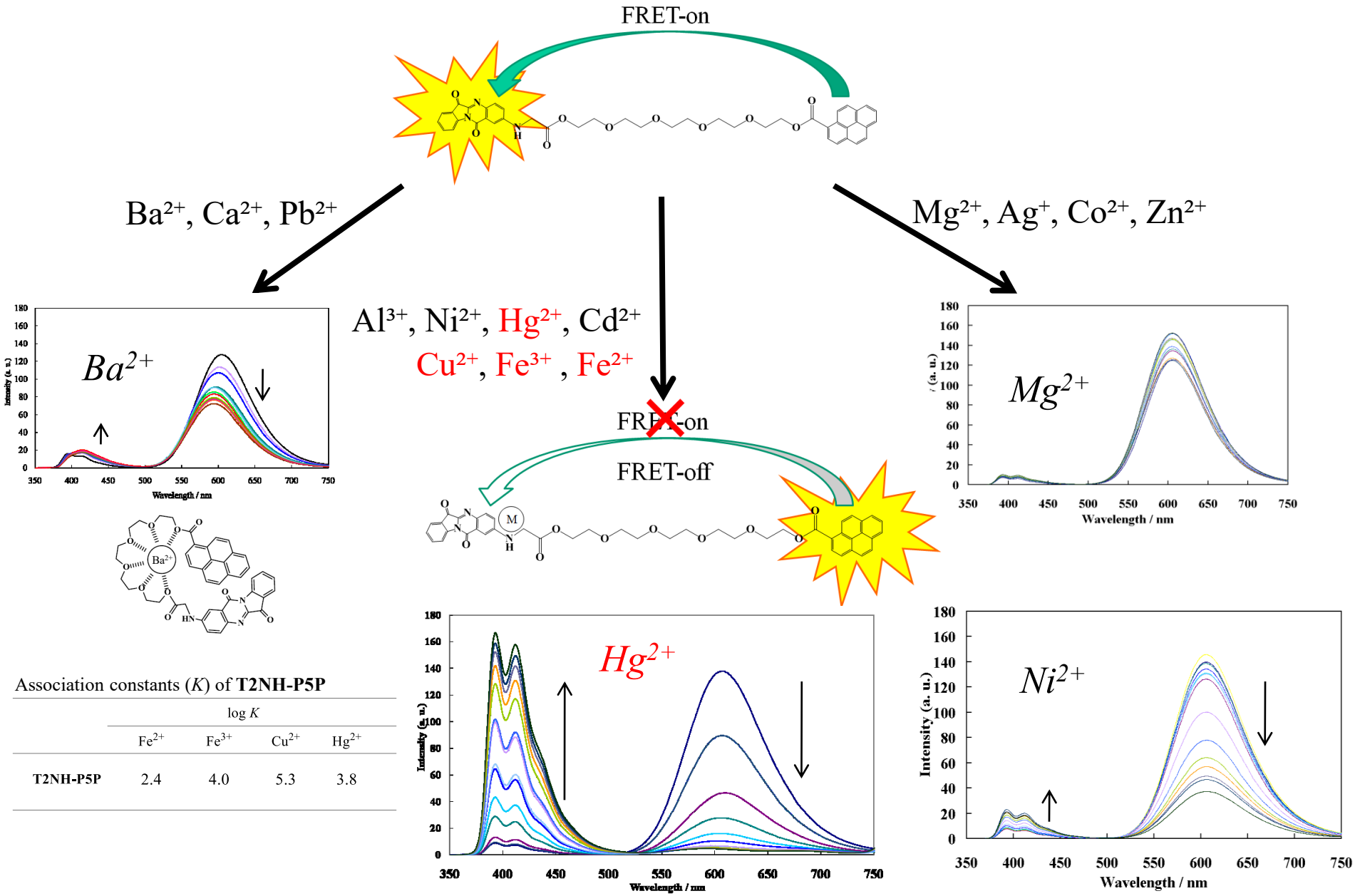

Association constants (K) of **T2NH-P5P**

	log K			
	Fe^{2+}	Fe^{3+}	Cu^{2+}	Hg^{2+}
T2NH-P5P	2.4	4.0	5.3	3.8

Fluorescence spectra of **T2NH-P5P** (10 mM) upon addition of several metal ions (0 – 1000 equiv) in acetonitrile.

J. Kawakami, A. Soma, K. Kikuchi, Y. Kikuchi, S. Ito and H. Kitahara, *Anal. Sci.*, **2014**, *30*, 949-954.

Aliphatic protons

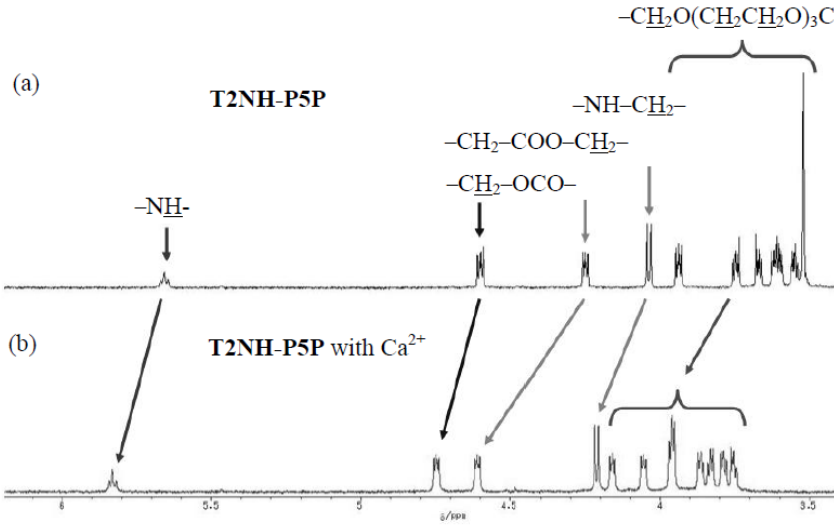

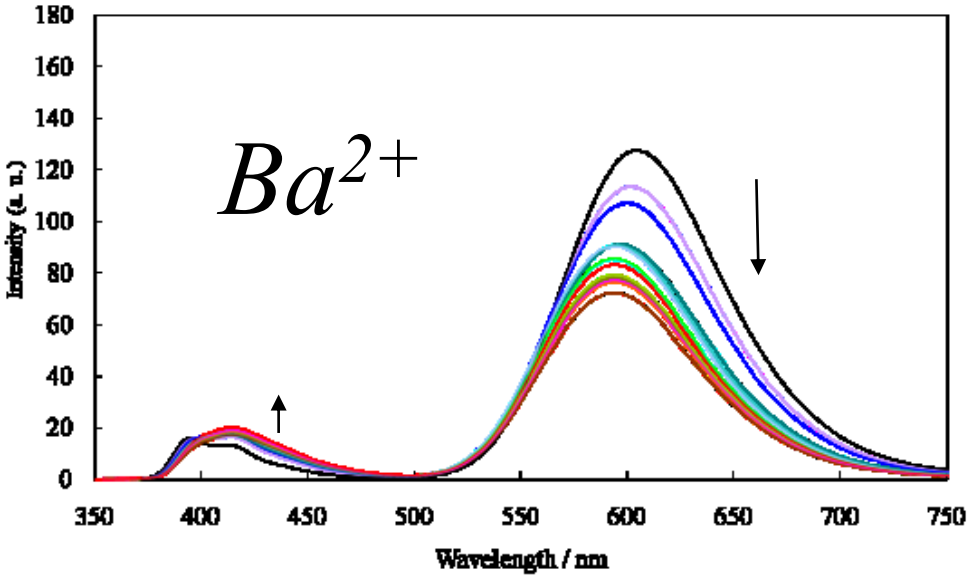

Aromatic protons

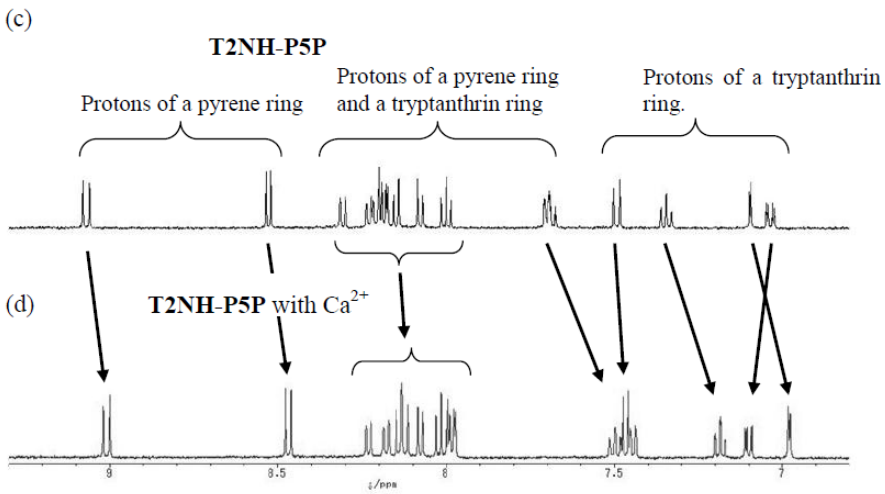

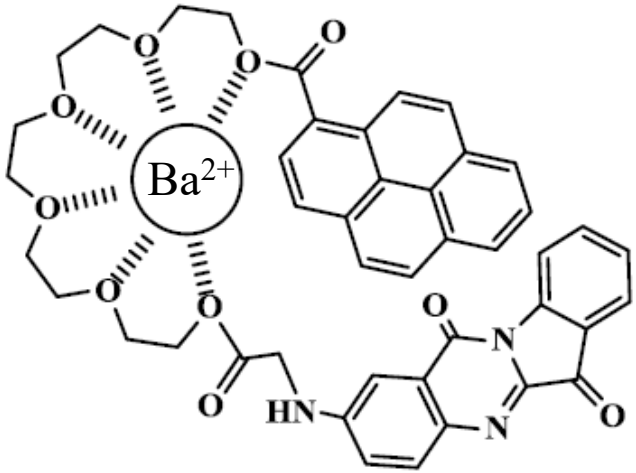

^{1}H NMR spectra of **T2NH-P5P** without (a and c) and with (b and d) calcium salt in acetonitrile-d_3 at room temperature.

J. Kawakami, A. Soma, K. Kikuchi, Y. Kikuchi, S. Ito and H. Kitahara, *Anal. Sci.*, **2014**, *30*, 949-954.

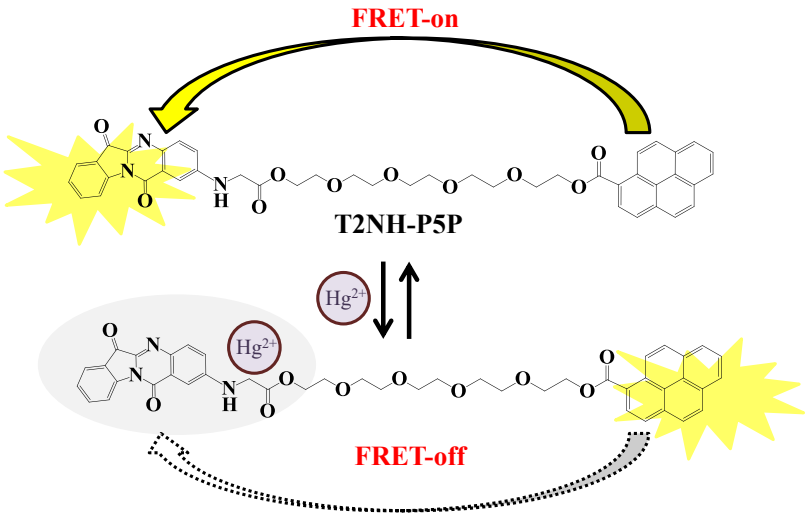

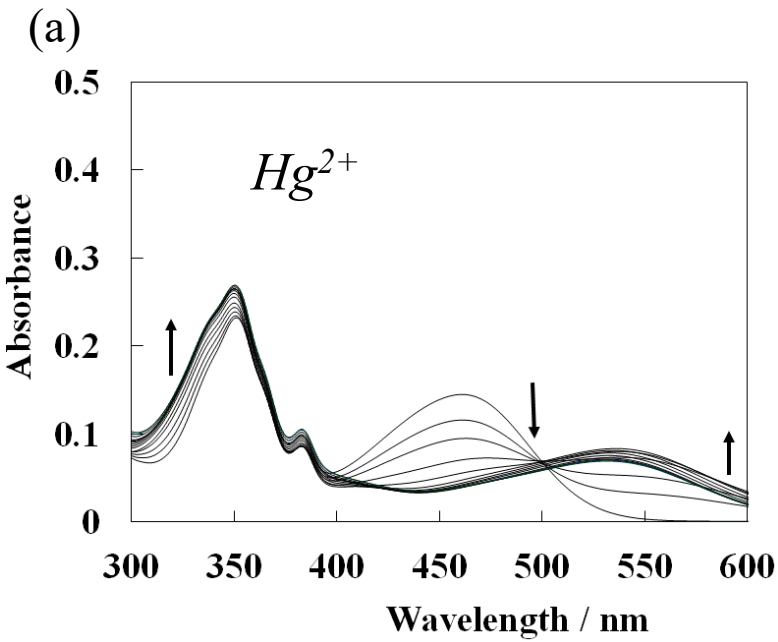

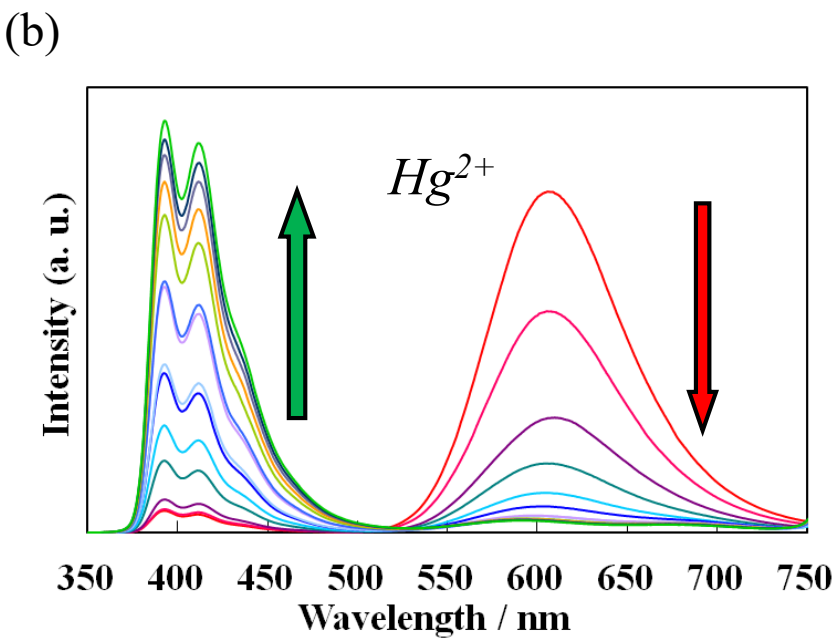

Spectral changes in the UV–vis absorption (a) and fluorescence (b) of **T2NH-P5P** (10 mM) upon addition of $Hg(ClO_4)_2$ (0 – 1000 equiv) in acetonitrile.

J. Kawakami, A. Soma, K. Kikuchi, Y. Kikuchi, S. Ito and H. Kitahara, *Anal. Sci.*, **2014**, *30*, 949-954 (Hot Article Award).

Optical window

The near-infrared (NIR) region (650–900 nm) is referred to as the "optical window" of cells and tissues because of the lack of efficient endogenous absorbers in this spectral range and the subsequent high penetration depth (of the order of a few millimeters) in most tissues.

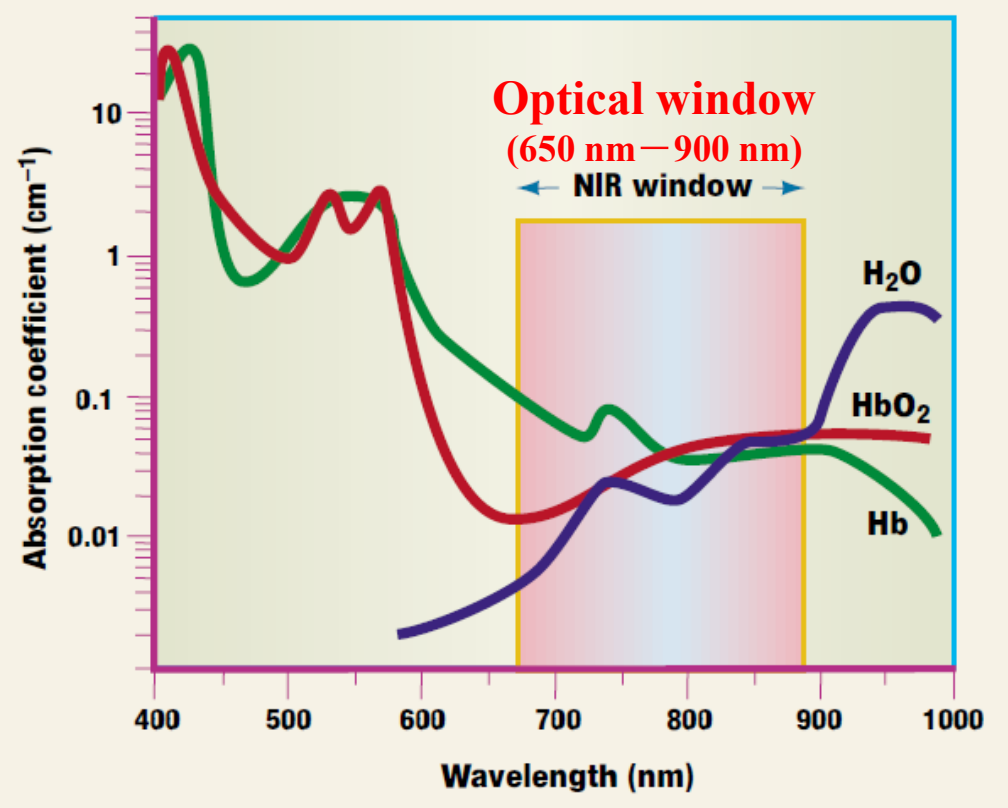

R. Weissleder, *Nat. Biotechnol.*, **19**, 316–317 (2001).

Fluorescent spectra of $T2NH_2$

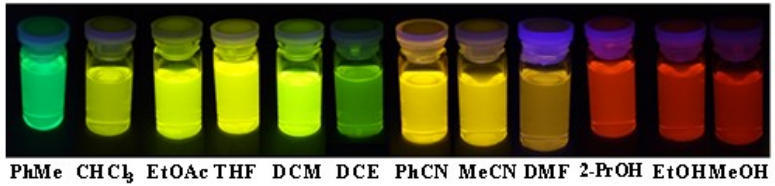

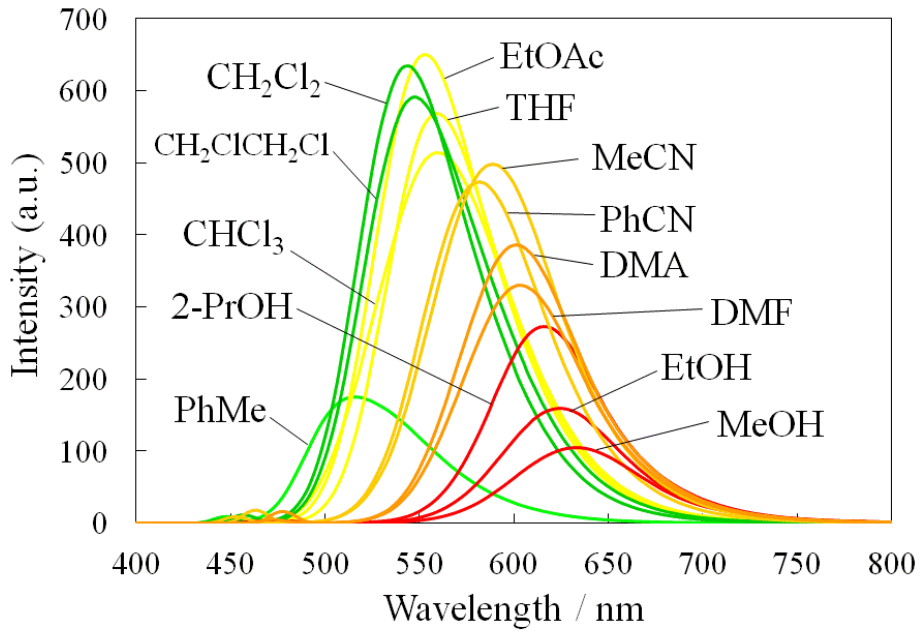

Florescence spectra in solvents of different polarity of **$T2NH_2$**.

Absorption maxima ($\lambda_{a,\,max}$), molar absorption coefficients ($\varepsilon_{a,\,max}$), emission maxima ($\lambda_{f,\,max}$), fluorescence quantum yields (Φ_f), and Stokes shifts of **$T2NH_2$**.

Solvents	$\lambda_{a,\,max}$ /	$\log(\varepsilon_{a,\,max}$ /	$\lambda_{f,\,max}$	Φ_f	Stokes shifts /cm^{-1}
	$T2NH_2$	**$T2NH_2$**	**$T2NH_2$**	**$T2NH_2$**	**$T2NH_2$**
PhMe	447	3.97	516	0.18	2992
$CHCl_3$	450	4.03	560	0.60	4365
EtOAc	452	4.12	553	0.67	4041
THF	457	4.08	558	0.59	3961
DCM	447	4.07	545	0.64	4023
DCE	447	4.05	547	0.64	4090
PhCN	462	4.16	581	0.51	4433
MeCN	451	4.13	588	0.56	5166
DMF	472	4.02	602	0.31	4575
DMSO	477	4.06	615	0.30	4704
2-PrOH	481	4.21	616	0.28	4556
EtOH	475	4.24	624	0.17	5027
MeOH	464	4.19	632	0.12	5729

J. Kawakami, H. Kawaguchi, K. Kikuchi, A. Yamaya, S. Ito and H. Kitahara, *Trans. Mater. Res. Soc. Japan*, **2013**, *38*, 123-125.

Synthesis of 2-(4-aminophenyl)tryptanthrin derivatives

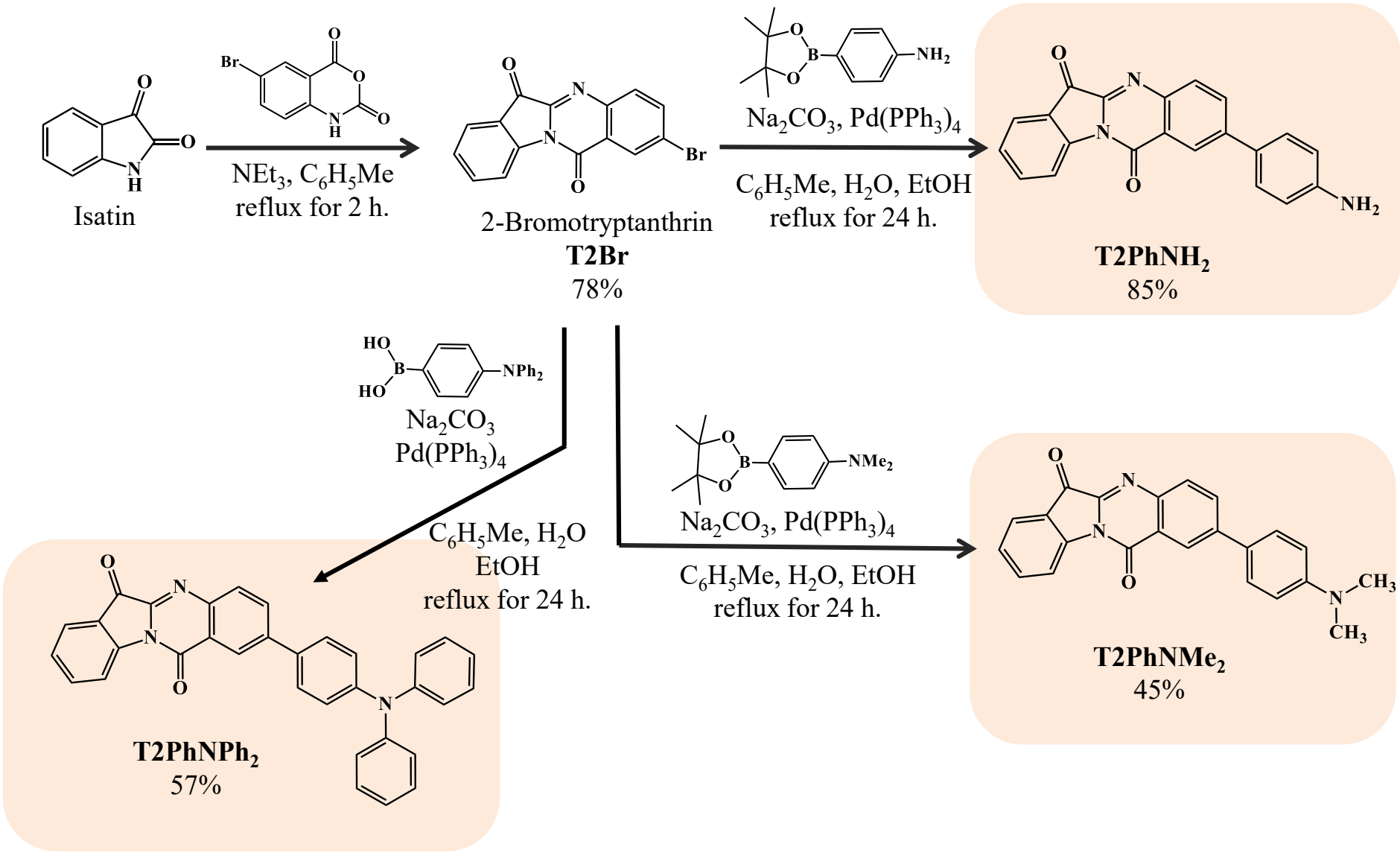

Absorption spectra of $T2NH_2$, $T2PhNH_2$, $T2PhNMe_2$ and $T2PhNPh_2$

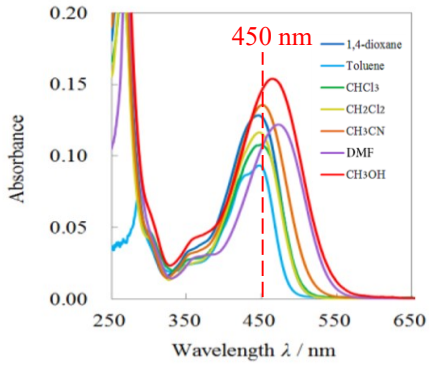

$T2NH_2$

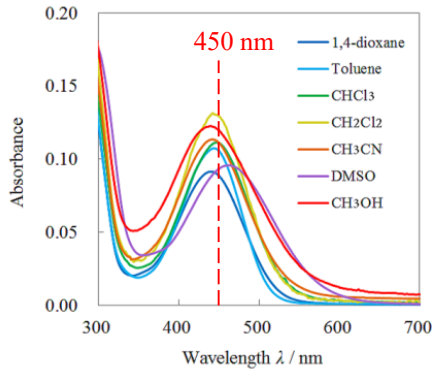

$T2PhNH_2$

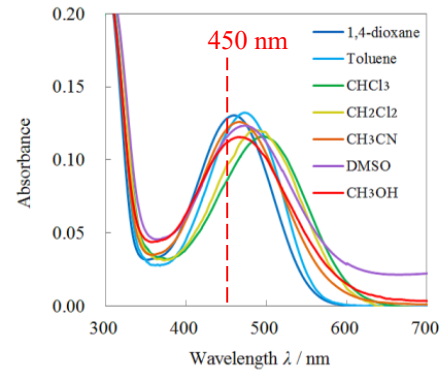

$T2PhNMe_2$

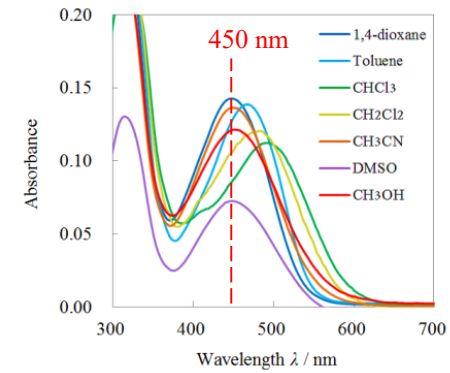

$T2PhNPh_2$

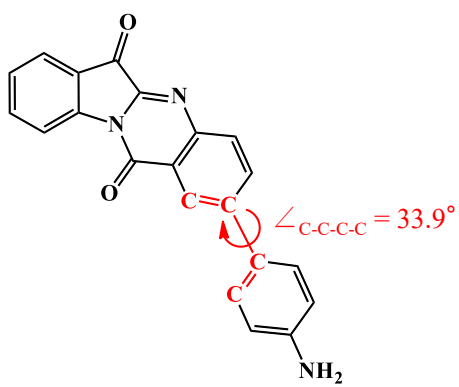

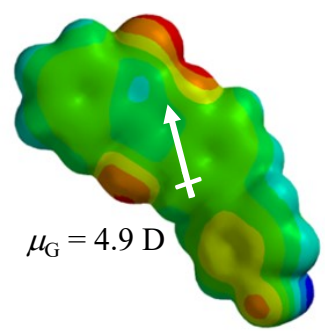

Electrostatic Potential Map

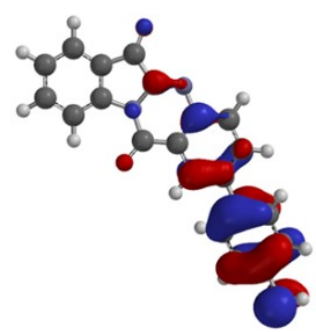

HOMO

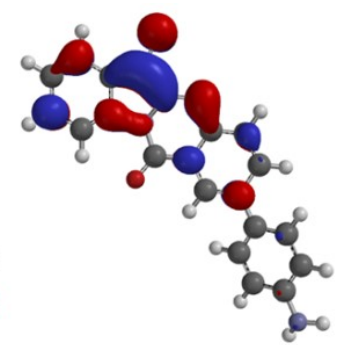

LUMO

Molecular properties of **$T2PhNH_2$** by DFT calculation (B3LYP 6-31G(d), in vacuum).

Fluorescence spectra of $T2NH_2$, $T2PhNH_2$, $T2PhNMe_2$ and $T2PhNPh_2$

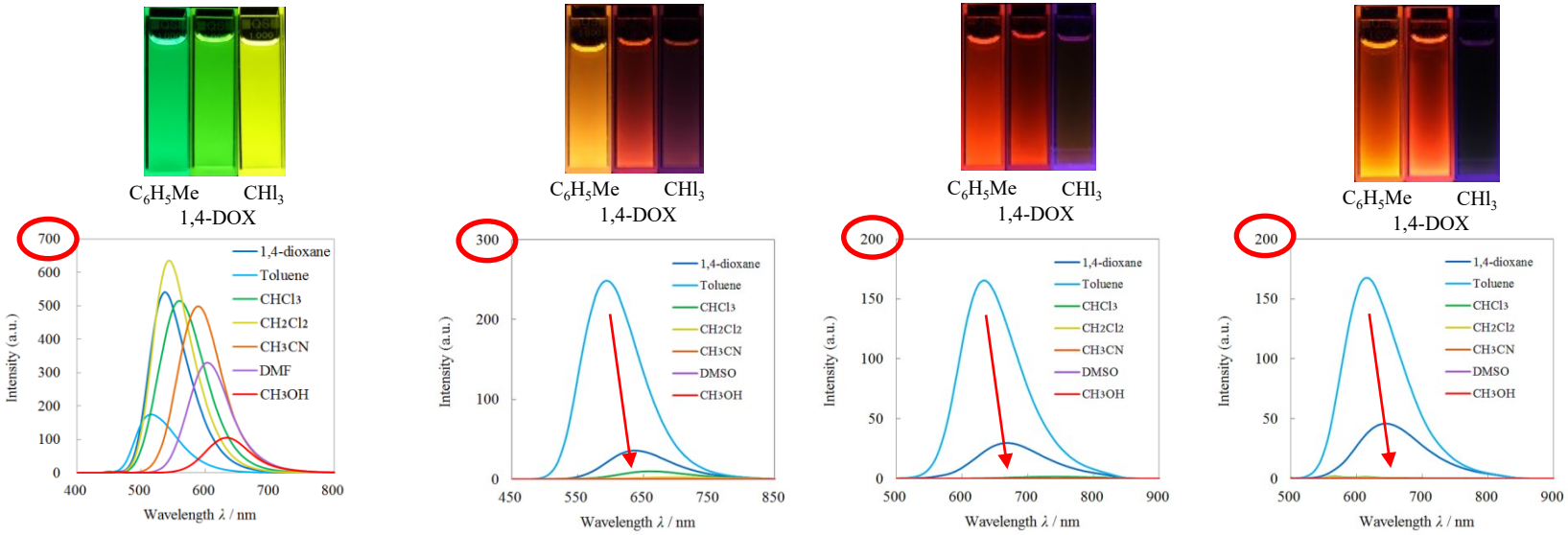

$T2NH_2$ **$T2PhNH_2$** **$T2PhNMe_2$** **$T2PhNPh_2$**

$$\Delta\lambda = \lambda_{f,\,max,\,\mathbf{T2PhNR_2}} - \lambda_{f,\,max,\,\mathbf{T2NH_2}} = 78\sim117 \text{ nm in Toluene}$$

solvent	$T2NH_2$			$T2PhNH_2$			$T2PhNMe_2$			$T2PhNPh_2$		
	$\lambda_{a,\,max}$	$\lambda_{f,\,max}$	Φ_f	$\lambda_{a,\,max}$	$\lambda_{f,\,max}$	Φ_f	$\lambda_{a,\,max}$	$\lambda_{f,\,max}$	Φ_f	$\lambda_{a,\,max}$	$\lambda_{f,\,max}$	Φ_f
1,4-dioxane	440	537	0.47	440	639	0.06	460	669	0.05	448	645	0.08
Toluene	447	516	0.18	444	594	0.36	474	633	0.25	468	617	0.24
$CHCl_3$	450	560	0.60	448	662	0.02	497	744	<0.01	492	613	<0.01
CH_2Cl_2	447	545	0.64	442	694	<0.01	489	793	<0.01	482	612	<0.01
CH_3CN	451	588	0.56	442	—	—	466	—	—	450	—	—
DMSO	477	615	0.30	462	—	—	474	—	—	449	—	—
CH_3OH	464	632	0.12	440	—	—	466	—	—	452	—	—

Quenching mechanism of T2PhNR$_2$ in polar solvents.

Intersystem crossing of **T2PhNH$_2$** from S_1 to T_1 is a forbidden transition by El-Sayed rule.

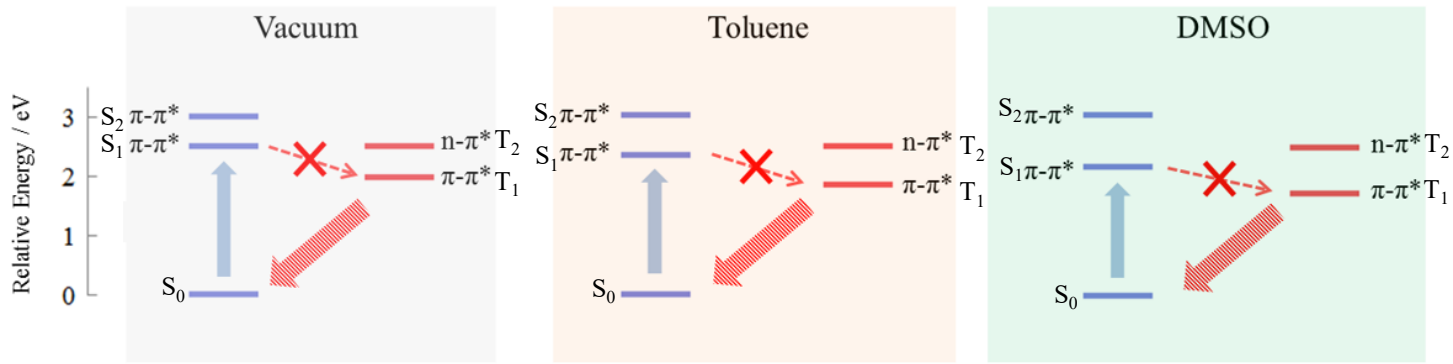

S_n (n = 1, 2) and T_n (n = 1, 2) energies of **T2PhNH$_2$** by TDDFT calculations (B3LYP 6-31+G*) in vacuum, toluene and DMSO.

M. A. El-Sayed, *J. Chem. Phys.*, **1963**, *38*, 2834–2838.

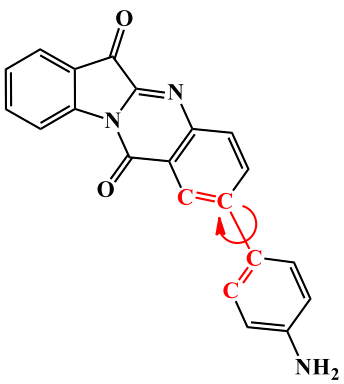

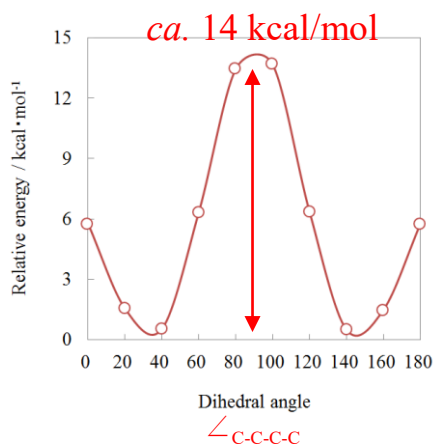

Rotational energy barriers	
H_3C—CH_3	*ca.* 3 kcal/mol
H_3CH_2C—CH_2CH_3	*ca.* 5 kcal/mol
H_2C=CH_2	*ca.* 65 kcal/mol

The rotational energy barrier of **T2hNH$_2$** in the grand-state by DFT calculation (B3LYP 6-31G(d), in vacuum).

Synthesis of benzo-fused 2-aminotriptanthrin ($BF\text{-}T2NH_2$) and naphthalene-fused 2-aminotriptanthrin ($NF\text{-}T2NH_2$)

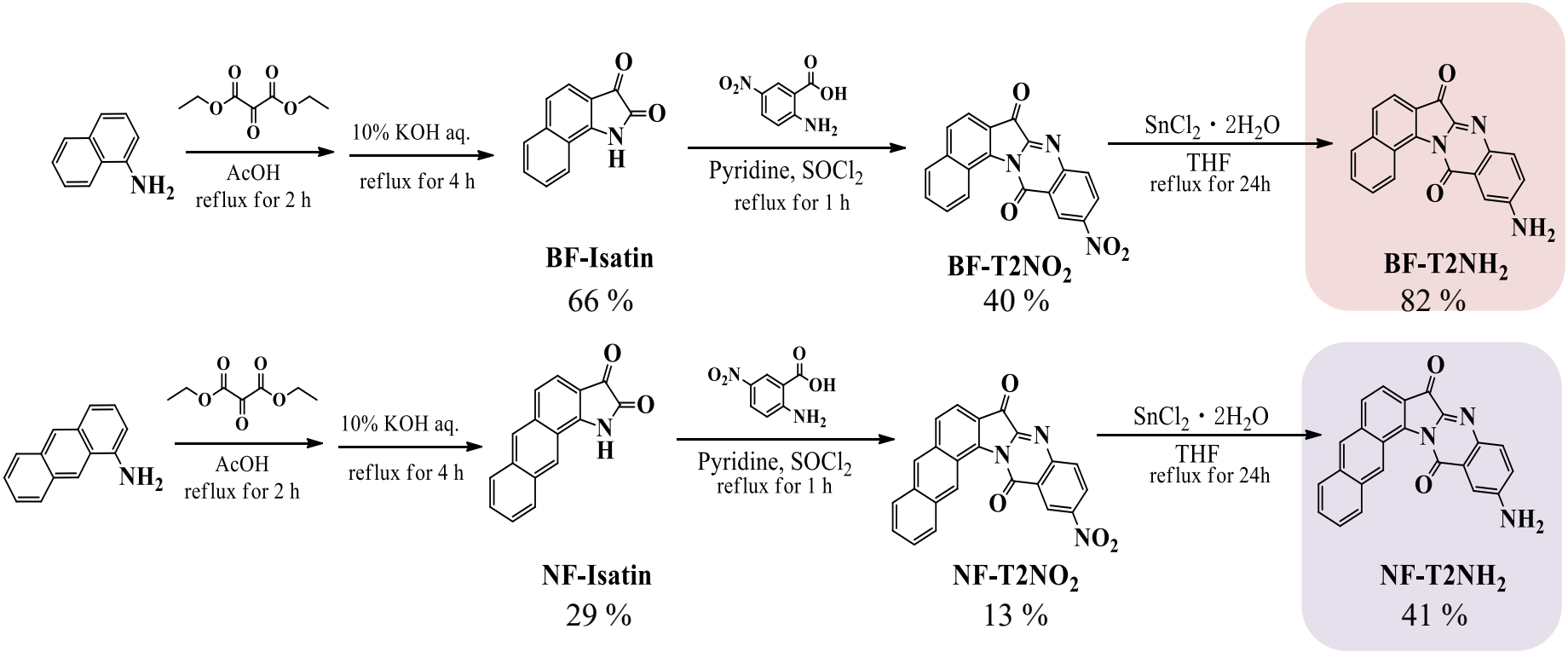

Absorption and fluorescence spectra of $T2NH_2$, $BF\text{-}T2NH_2$, and $NF\text{-}T2PhNH_2$

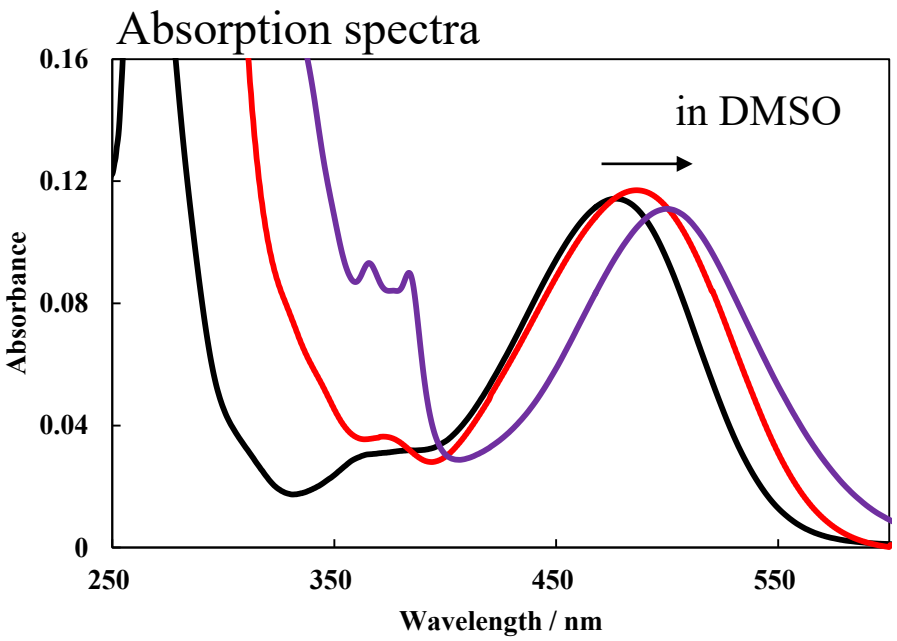

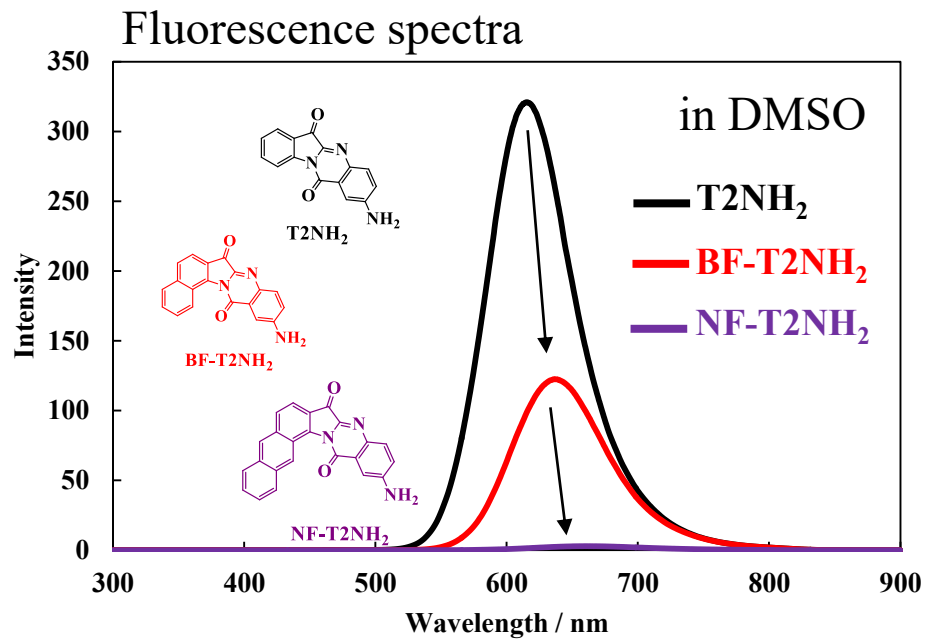

Solvents	$\lambda_{a,\,max}$ / nm			$\lambda_{f,\,max}$ / nm			Φ_f		
	$T2NH_2$	$BF\text{-}T2NH_2$	$NF\text{-}T2NH_2$	$T2NH_2$	$BF\text{-}T2NH_2$	$NF\text{-}T2NH_2$	$T2NH_2$	$BF\text{-}T2NH_2$	$NF\text{-}T2NH_2$
PhMe	447	458	462	516	538	602	0.18	0.04	< 0.01
$CHCl_3$	450	459	469	560	579	578	0.60	0.02	< 0.01
EtOAc	452	462	475	553	573	602	0.67	0.20	< 0.01
THF	457	467	480	558	576	600	0.59	0.22	< 0.01
MeCN	451	463	476	588	608	604	0.56	0.26	< 0.01
DMF	472	481	493	602	625	648	0.31	0.20	< 0.01
DMSO	477	486	500	615	637	661	0.30	0.19	< 0.01
EtOH	475	485	499	624	643	641	0.17	0.10	< 0.01
MeOH	464	475	491	632	653	646	0.12	0.05	< 0.01

LUMO

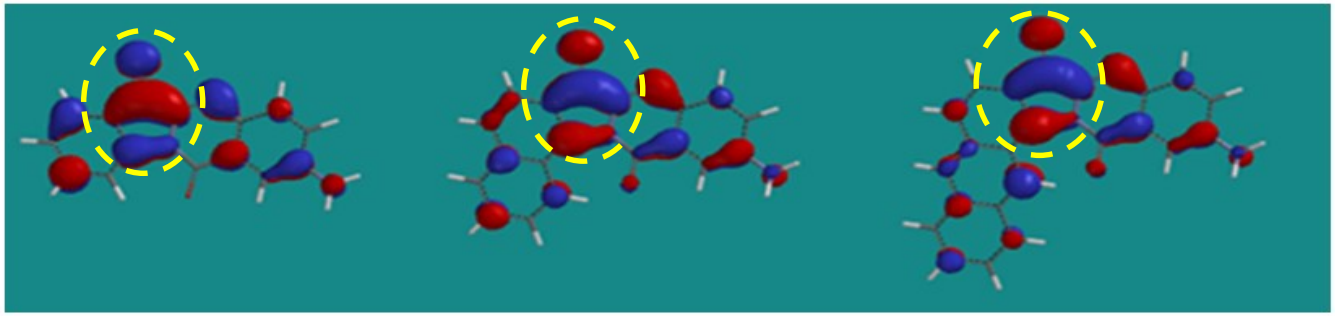

HOMO

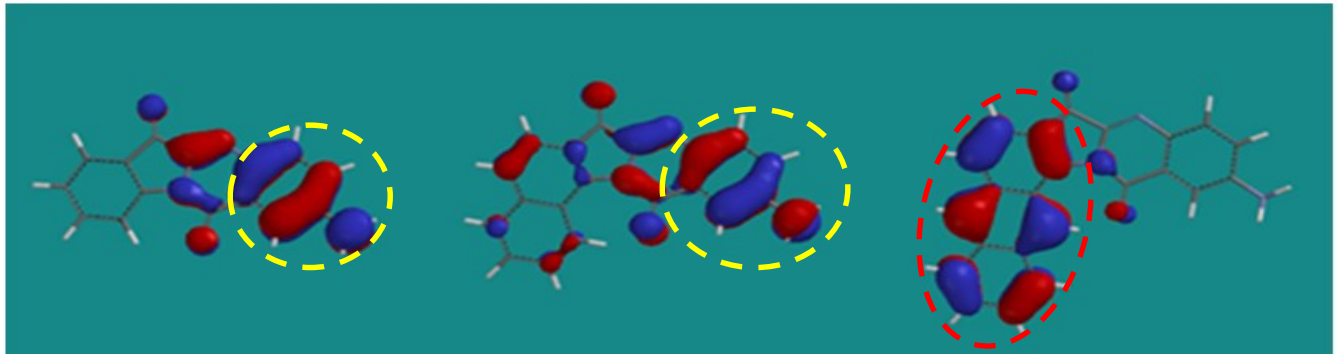

T2NH$_2$ **BF-T2NH$_2$** **NF-T2NH$_2$**

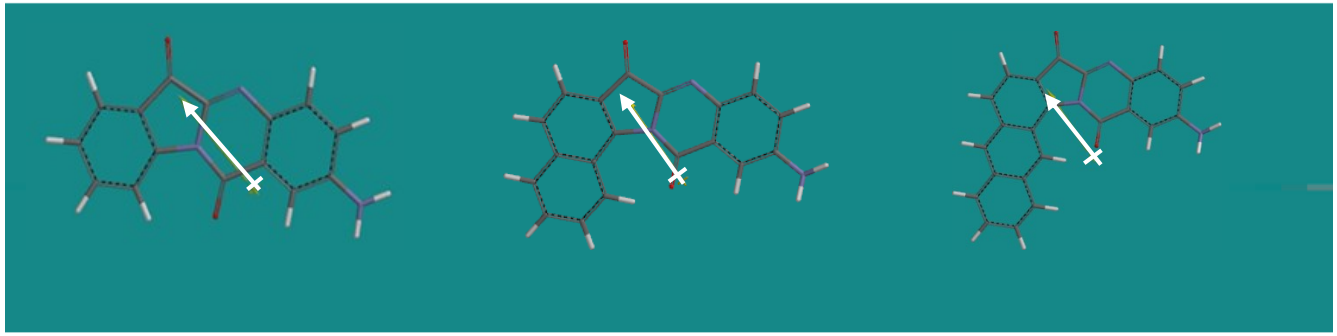

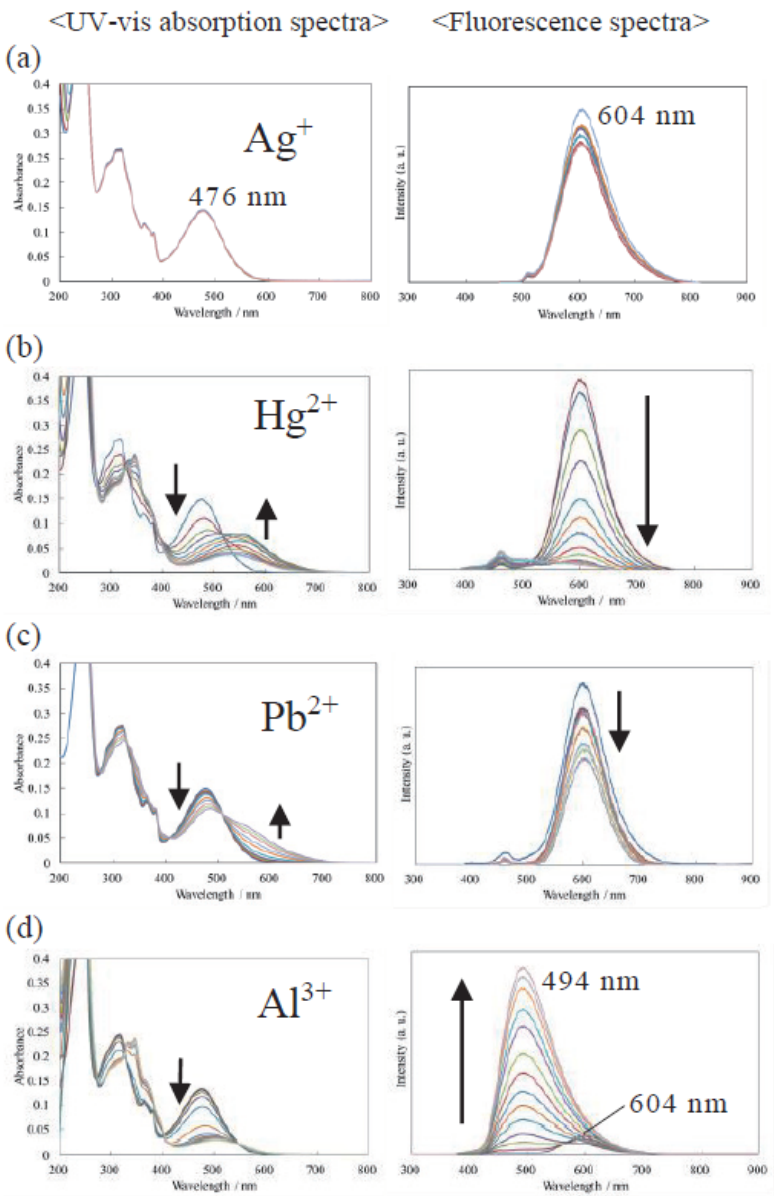

Mg^{2+}, Ca^{2+}, Ba^{2+}, Co^{2+}, Ag^{+}, Zn^{2+}, and Cd^{2+}

Fe^{2+}, Fe^{3+}, Ni^{2+}, Cu^{2+}, Hg^{2+}, and Pb^{2}

Al^{3+}

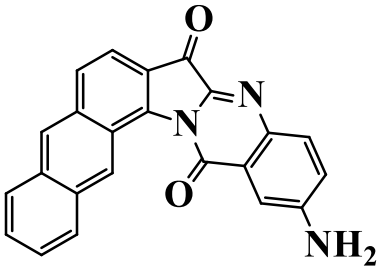

NF-T2NH$_2$

UV–vis absorption and florescence spectra of **NF-T2NH$_2$** with (a) Ag^{+}, (b) Hg^{+}, (c) Pb^{2+}, and (d) Al^{3+} in acetonitrile: [**NF-T2NH$_2$**] = 10 μM, Ag^{+}, Hg^{+}, Pb^{2+}, and Al^{3+} = 0–1000 equiv.

J. Kawakami, A. Tsuiki, S. Ito, and H. Kitahara, *Trans. Mater. Res. Soc. Japan*, **2016**, *41*, 131-133.

Accelerating ICT

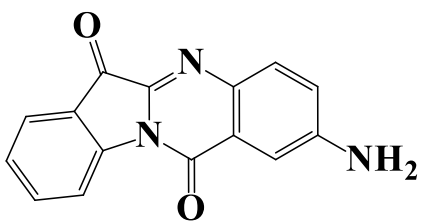

T2NH$_2$

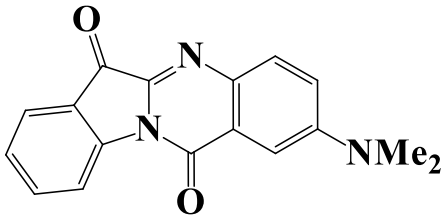

T2NMe$_2$

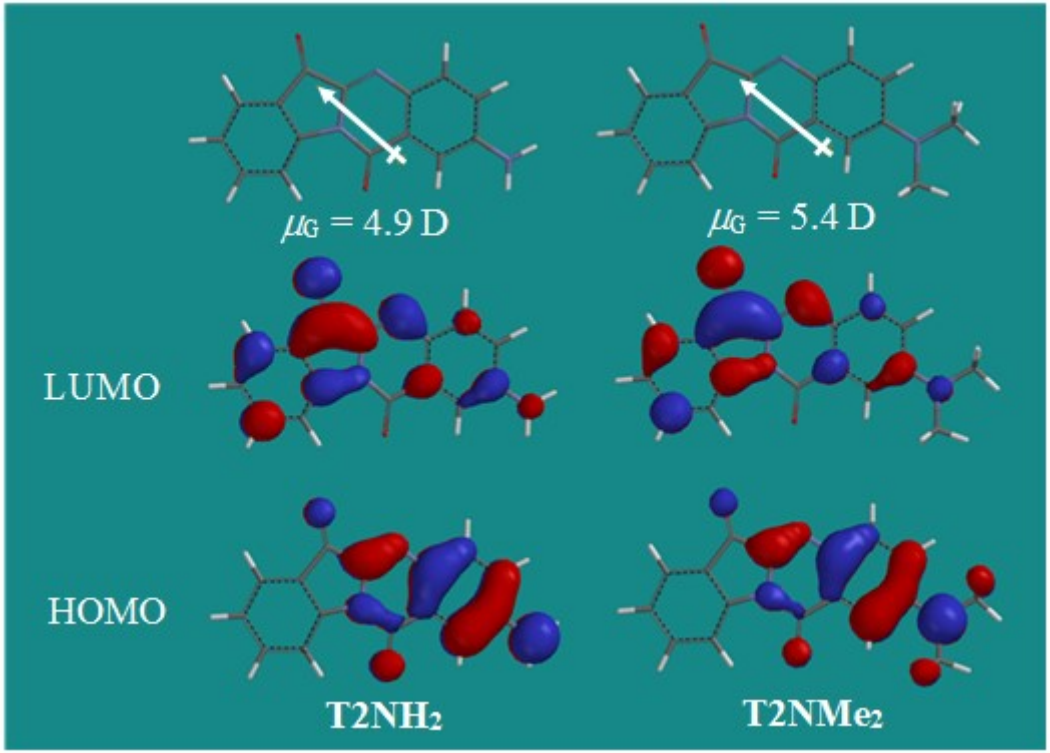

HOMO and LUMO surfaces and μ_G values of **T2NH$_2$** and **T2NMe$_2$** according to DFT calculations.

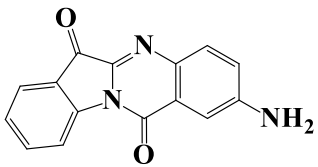

T2NH$_2$

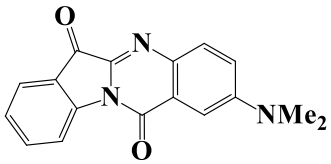

T2NMe$_2$

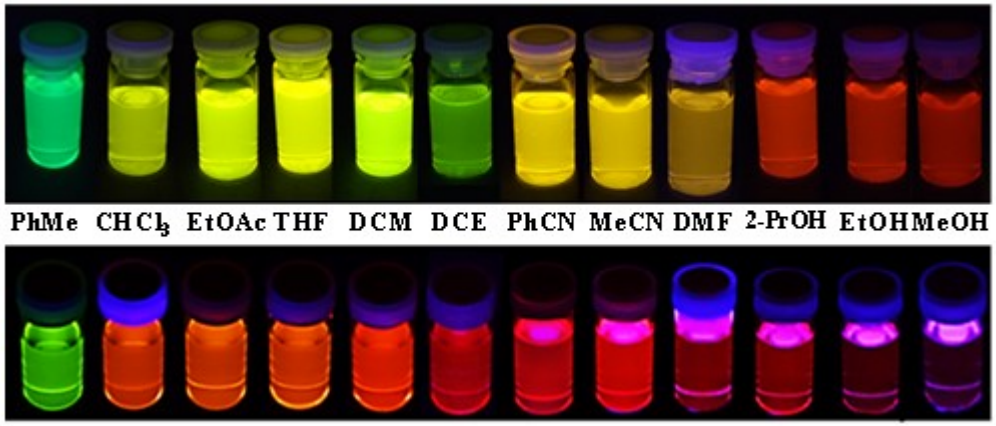

Photographs of **T2NH$_2$** and **T2NMe$_2$** taken under 365 nm UV light in different solvents.

Absorption maxima ($\lambda_{a,\ max}$), molar absorption coefficients ($\varepsilon_{a,\ max}$), emission maxima ($\lambda_{f,\ max}$), fluorescence quantum yields (Φ_f), and Stokes shifts of **T2NH$_2$** and **T2NMe$_2$**[6].

Solvents	$\lambda_{a,\ max}$ / nm		$\log(\varepsilon_{a,\ max}$ / dm^{-3} mol^{-1} cm^{-1})		$\lambda_{f,\ max}$ / nm		Φ_f		Stokes shifts /cm^{-1}	
	T2NH2	**T2NMe2**	**T2NH2**	**T2NMe2**	**T2NH2**	**T2NMe2**	**T2NH2**	**T2NMe2**	**T2NH2**	**T2NMe2**
PhMe	447	488	3.97	4.34	516	551	0.18	0.90	2992	2343
$CHCl_3$	450	508	4.03	4.34	560	592	0.60	0.96	4365	2793
EtOAc	452	481	4.12	4.29	553	596	0.67	0.79	4041	4011
THF	457	481	4.08	4.27	558	595	0.59	0.82	3961	3983
DCM	447	503	4.07	4.35	545	604	0.64	0.89	4023	3324
DCE	447	499	4.05	4.18	547	608	0.64	0.88	4090	3593
PhCN	462	504	4.16	4.32	581	624	0.51	0.51	4433	3816
MeCN	451	490	4.13	4.29	588	637	0.56	0.28	5166	4710
DMF	472	492	4.02	4.26	602	641	0.31	0.17	4575	4725
DMSO	477	496	4.06	4.21	615	654	0.30	0.12	4704	4871
2-PrOH	481	496	4.21	4.24	616	650	0.28	0.15	4556	4777
EtOH	475	497	4.24	4.22	624	660	0.17	0.08	5027	4969
MeOH	464	493	4.19	4.25	632	674	0.12	0.04	5729	5447

J. Kawakami, T. Kadowaki, M. Ikeda, Y. Habata, S. Ito and H. Kitahara, *Trans. Mater. Res. Soc. Japan*, **2016**, *41*, 143-143.

Lippert–Mataga plots

$$\Delta\nu = 2(\mu_E - \mu_G)^2 \Delta f / hca^3 + \text{constant} \qquad (1)$$
$$\Delta f = \{(\varepsilon - 1) / (2\varepsilon + 1)\} - \{(n^2 - 1) / (2n^2 + 1)\}$$

h (6.6256×10^{-27} erg s) is Planck's constant, c (2.9979×10^{10} cm s^{-1}) is the speed of light, a is the radius of the cavity in which the fluorophore resides, ν_A and ν_F are the wavenumbers (cm^{-1}) of the absorption and emission bands, respectively. Equation (1) describes the Stokes shifts ($\Delta\nu = \nu_A - \nu_F$) in terms of the change in dipole moment of the fluorophore ($\Delta\mu = \mu_E - \mu_G$) and the dependence of the dipole energy on the ε values and refractive index (n) of the solvent.

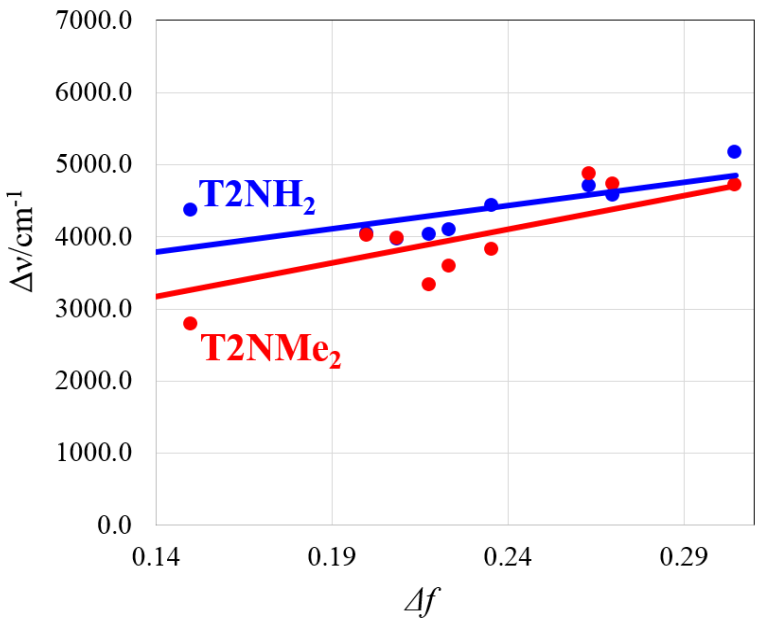

Lippert–Mataga plots of **T2NH$_2$** and **T2NMe$_2$** showing $\Delta\nu$ versus Δf.

Molecular radii[a)] and μ_G and μ_E values of **T2NH$_2$** and **T2NMe$_2$**.

	T2NH$_2$	**T2NMe$_2$**
a / Å [a)]	6.03	6.66
$\Delta\mu$ ($= \mu_E - \mu_G$) /D	11.9	16.5
μ_G /D[a)]	4.9	5.4
μ_E /D	16.8	21.9

a) Obtained from DFT calculations.

J. Kawakami, T. Kadowaki, M. Ikeda, Y. Habata, S. Ito and H. Kitahara, *Trans. Mater. Res. Soc. Japan*, **2016**, *41*, 143-143.

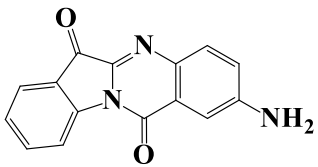

T2NH$_2$

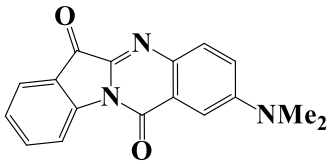

T2NMe$_2$

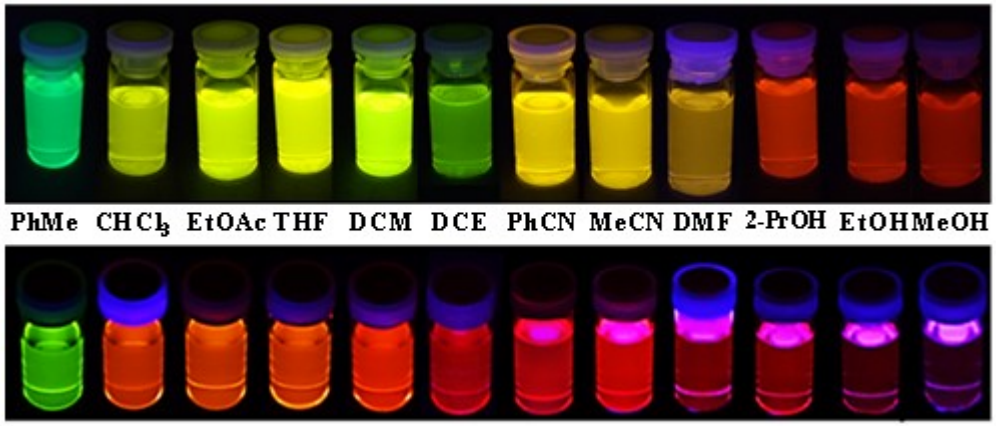

Photographs of **T2NH$_2$** and **T2NMe$_2$** taken under 365 nm UV light in different solvents.

Absorption maxima ($\lambda_{a,\ max}$), molar absorption coefficients ($\varepsilon_{a,\ max}$), emission maxima ($\lambda_{f,\ max}$), fluorescence quantum yields (Φ_f), and Stokes shifts of **T2NH$_2$** and **T2NMe$_2$**[6].

Solvents	$\lambda_{a,\ max}$ / nm		log($\varepsilon_{a,\ max}$ / dm^{-3} mol^{-1} cm^{-1})		$\lambda_{f,\ max}$ / nm		Φ_f		Stokes shifts /cm^{-1}	
	T2NH2	**T2NMe2**	**T2NH2**	**T2NMe2**	**T2NH2**	**T2NMe2**	**T2NH2**	**T2NMe2**	**T2NH2**	**T2NMe2**
PhMe	447	488	3.97	4.34	516	551	0.18	0.90	2992	2343
$CHCl_3$	450	508	4.03	4.34	560	592	0.60	0.96	4365	2793
EtOAc	452	481	4.12	4.29	553	596	0.67	0.79	4041	4011
THF	457	481	4.08	4.27	558	595	0.59	0.82	3961	3983
DCM	447	503	4.07	4.35	545	604	0.64	0.89	4023	3324
DCE	447	499	4.05	4.18	547	608	0.64	0.88	4090	3593
PhCN	462	504	4.16	4.32	581	624	0.51	0.51	4433	3816
MeCN	451	490	4.13	4.29	588	637	0.56	0.28	5166	4710
DMF	472	492	4.02	4.26	602	641	0.31	0.17	4575	4725
DMSO	477	496	4.06	4.21	615	654	0.30	0.12	4704	4871
2-PrOH	481	496	4.21	4.24	616	650	0.28	0.15	4556	4777
EtOH	475	497	4.24	4.22	624	660	0.17	0.08	5027	4969
MeOH	464	493	4.19	4.25	632	674	0.12	0.04	5729	5447

J. Kawakami, T. Kadowaki, M. Ikeda, Y. Habata, S. Ito and H. Kitahara, *Trans. Mater. Res. Soc. Japan*, **2016**, *41*, 143-143.

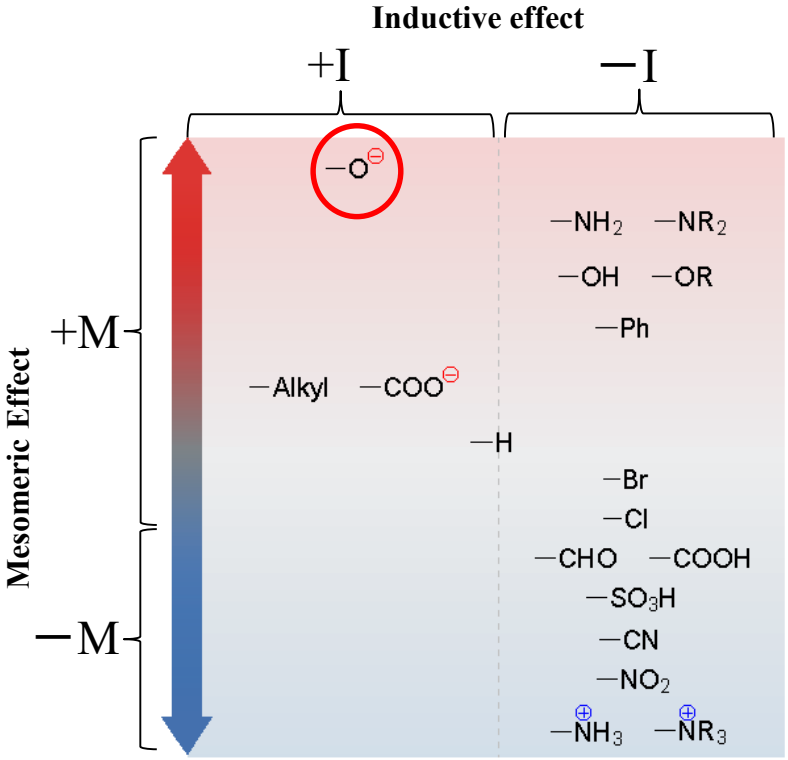

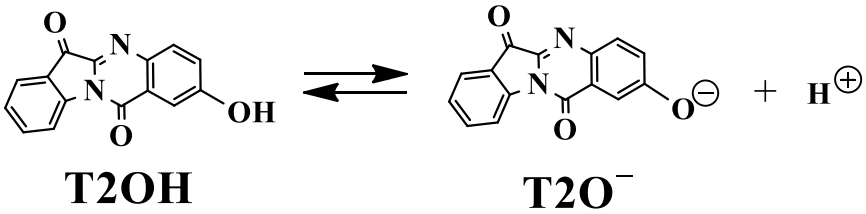

http://www.chemgapedia.de/vsengine/vlu/vsc/en/ch/12/oc/vlu_organik/aromaten/reaktionen/reaktionen_aromaten.vlu/Page/vsc/en/ch/12/oc/aromaten/reaktionen/ar_se/i_m_effekte/i_m_effekte.vscml.html

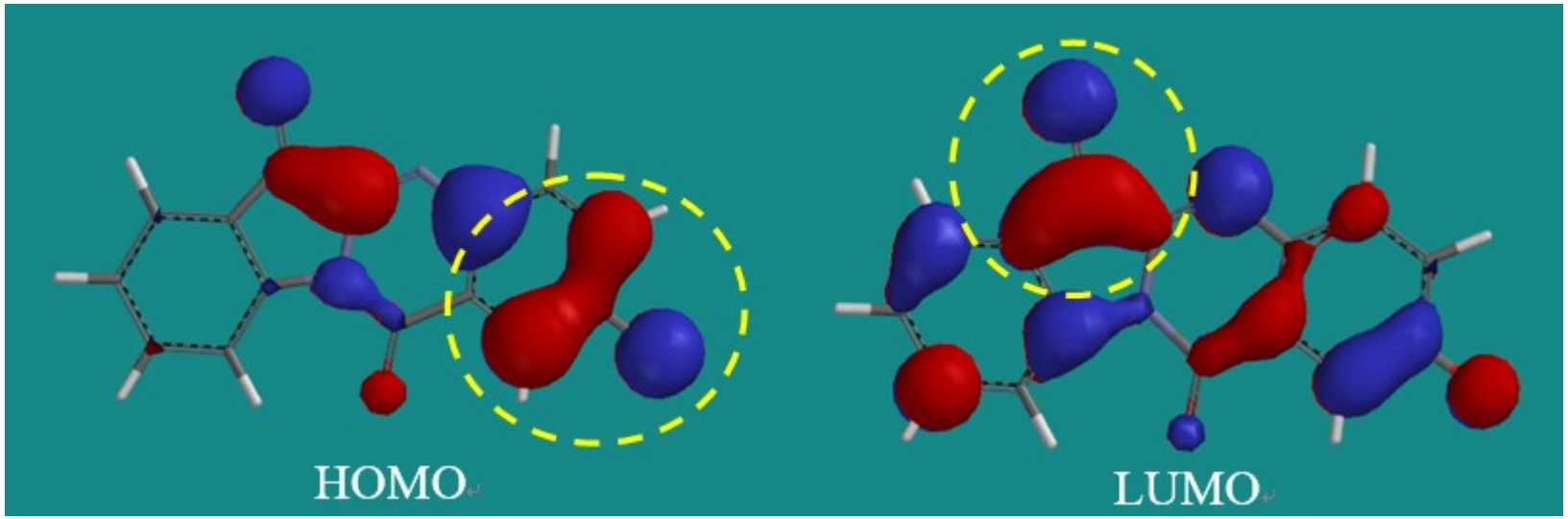

HOMO and LUMO surfaces of **T2O⁻** according to density functional theory calculations.

Absorption spectra of T2OH and T2ONa

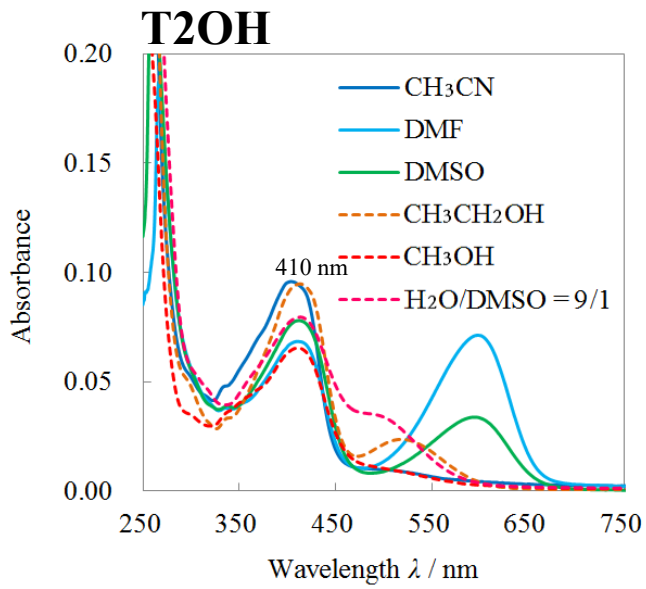

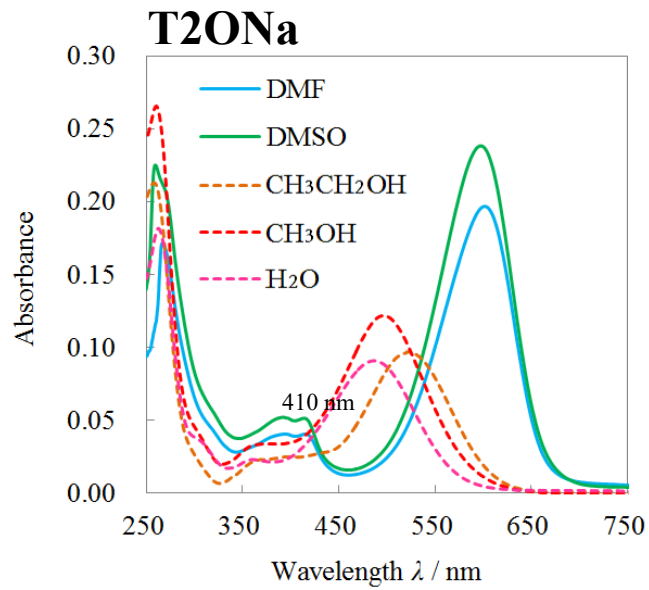

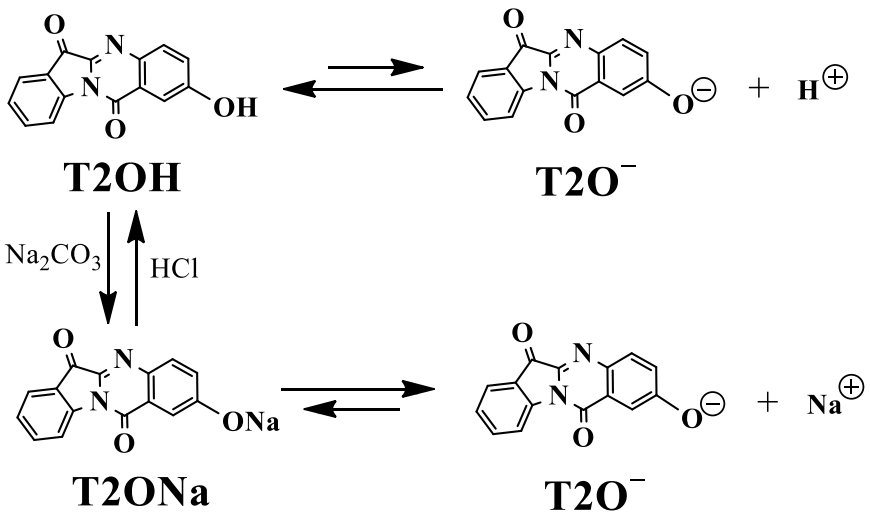

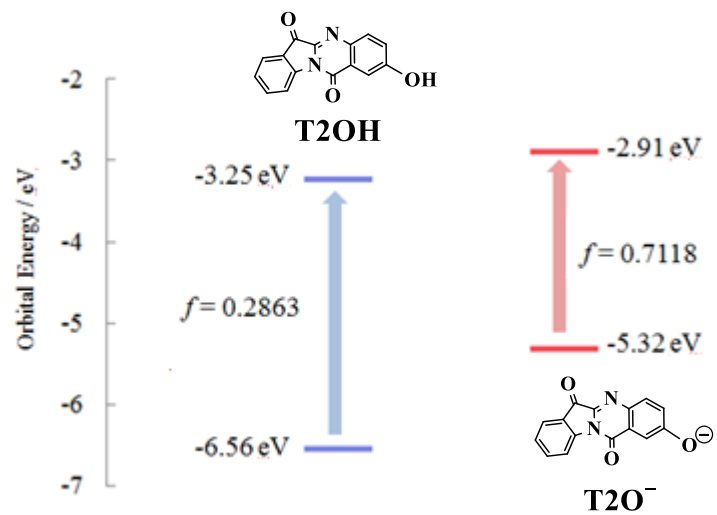

DFT calculations (B3LYP 6-31+G* in Acetone (**T2OH**) and DMSO (**T2O⁻**)).

Fluorescence spectra of T2OH and T2ONa

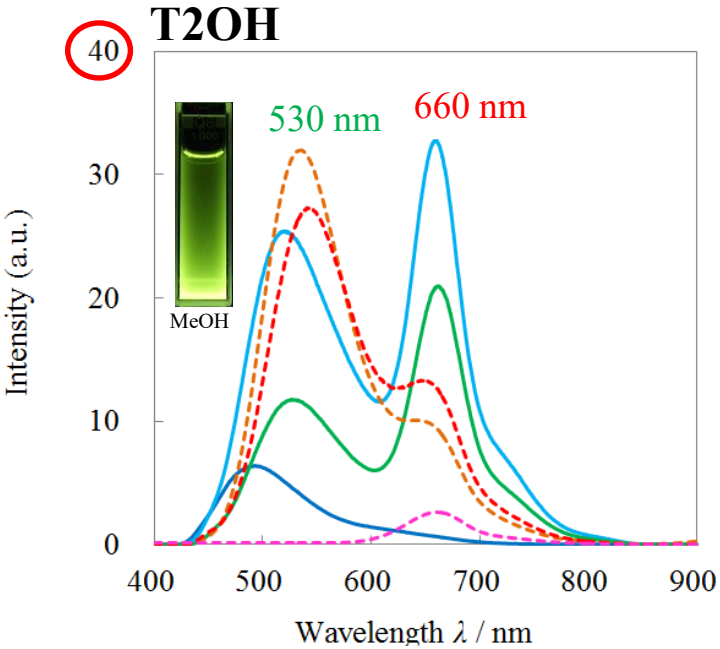

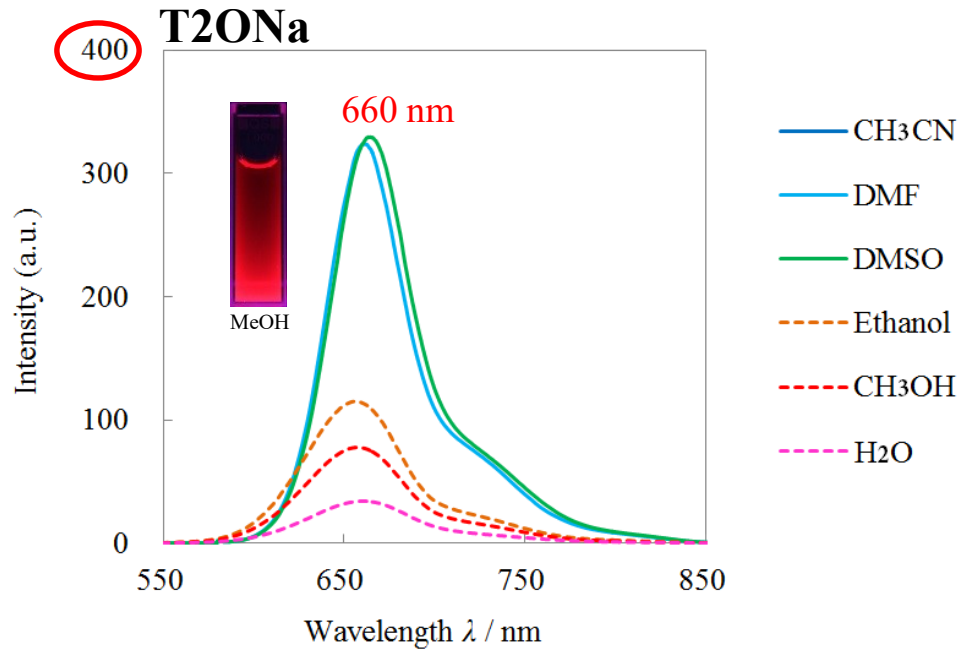

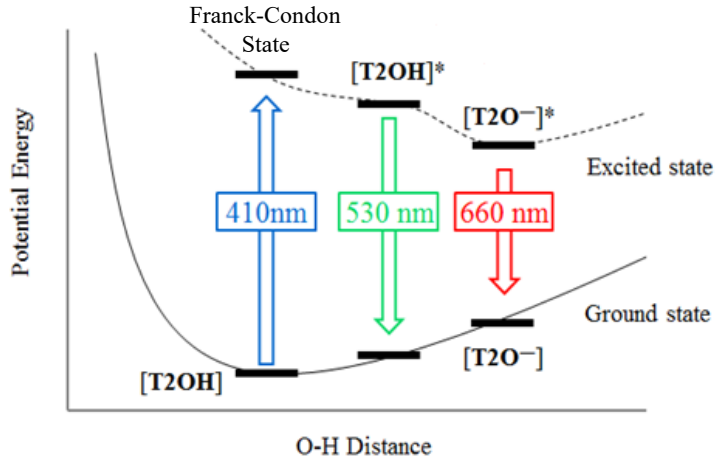

Solvents	$\lambda_{f,max}$ / nm		Φ_f	
	T2OH	**T2ONa**	**T2OH**	**T2ONa**
MeCN	493	not measured	0.01	not measured
DMF	522	662	0.06	0.36
DMSO	527	664	0.04	0.33
EtOH	533	656	0.05	0.09
MeOH	544	657	0.05	0.10
H_2O	611	662	< 0.01	0.04

pH-responsivity of T2OH

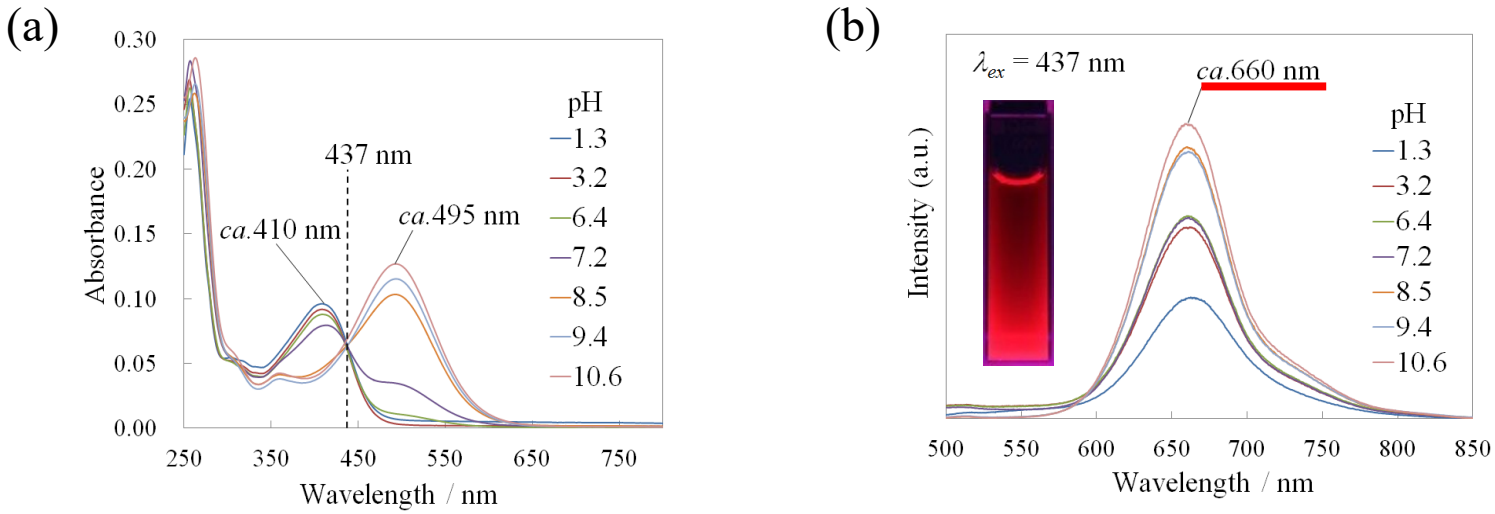

(a) UV-vis absorption and (b) fluorescence spectra of **T2OH** in a DMSO/H_2O (1/9, v/v) solution at different pH values.

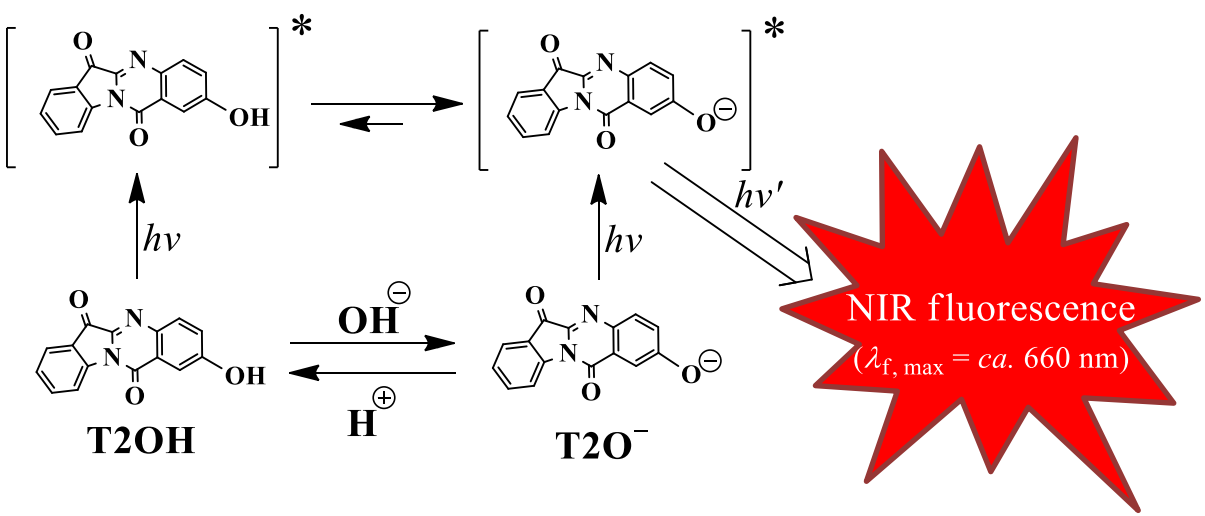

Compounds	pK_a	pK_a^*	
	Ground state	Excited state (Singlet)	Excited state (Triplet)
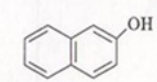	9.5	2.5	7.7
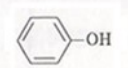	10.5	5.7	8.5

J. Kawakami, M. Takahashi, S. Ito, and H. Kitahara, *Anal. Sci.*, **2016**, *32*, 251-253.

Synthesis of T2OH, T2ONa and T2OAc

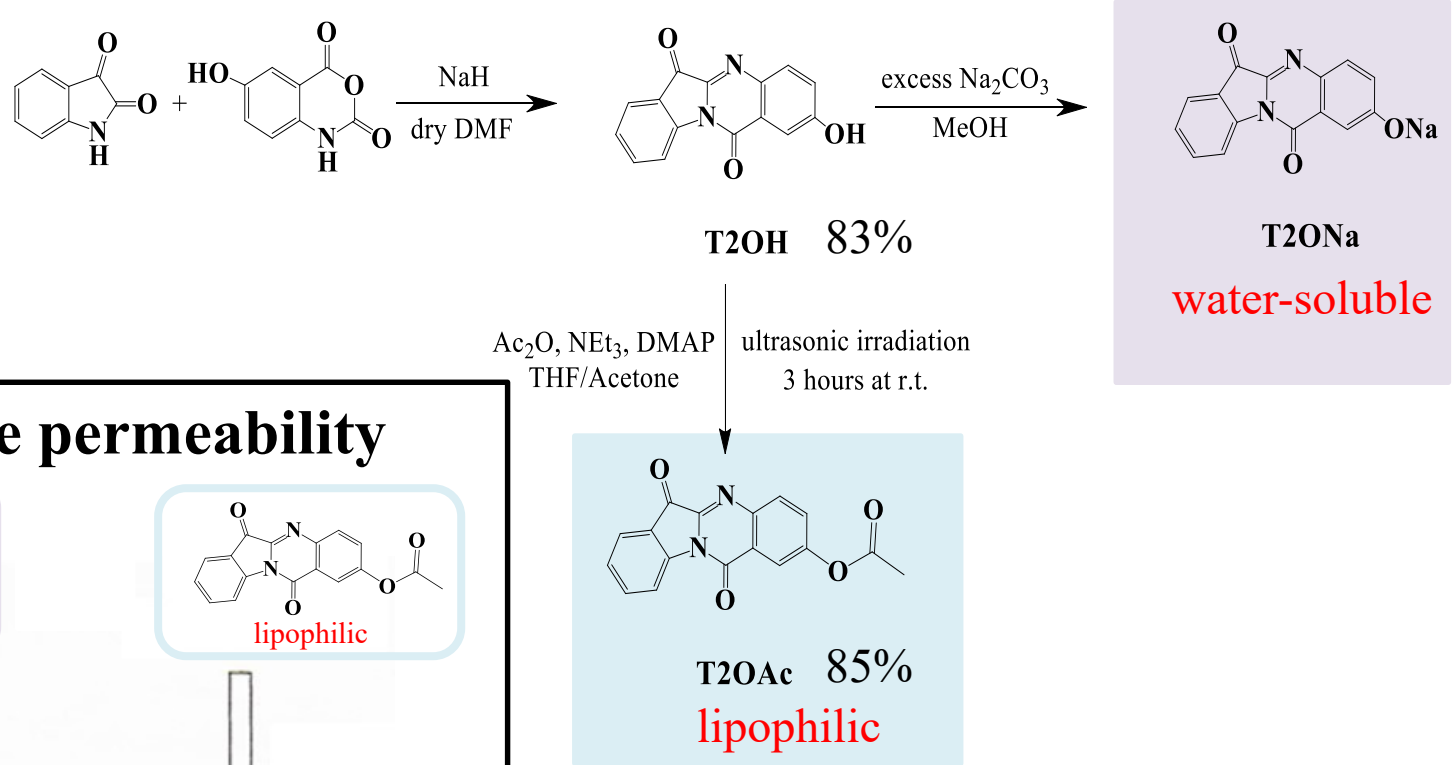

Cell membrane permeability

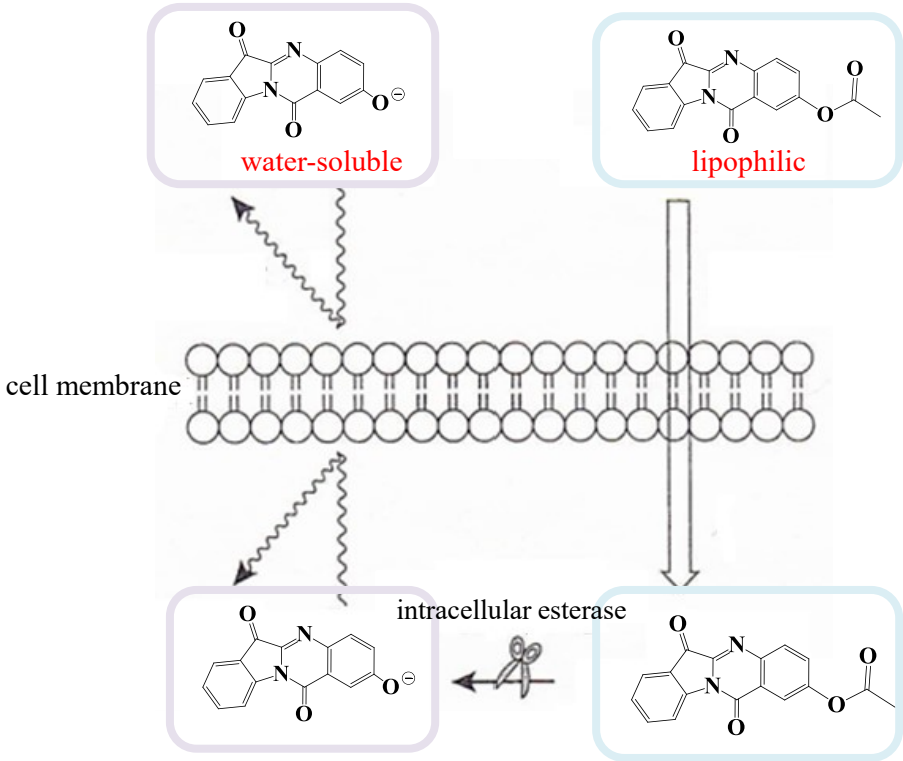

Absorption and fluorescence spectra of T2OH with TEA

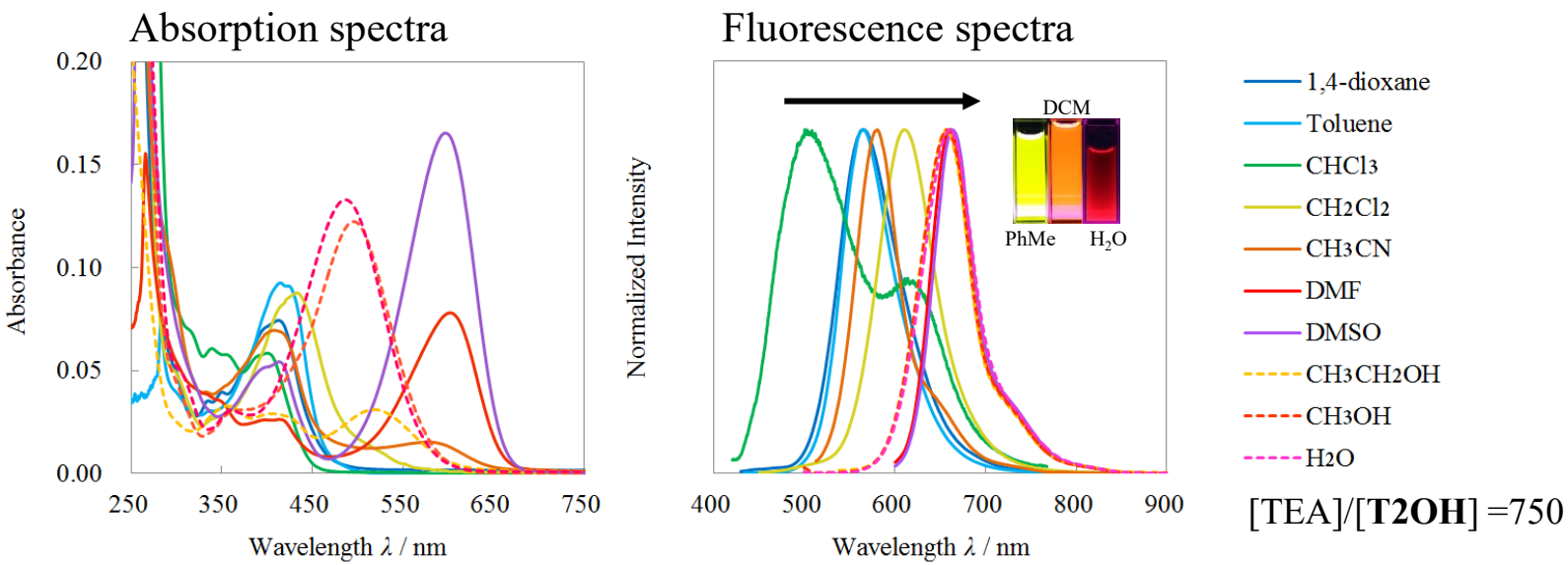

Solvents	$\lambda_{f,max}$ / nm		Φ_f	
	T2OH	**T2OH with TEA**	**T2OH**	**T2OH with TEA**
1,4-DOX	—	564	—	0.10
PhMe	—	565	—	0.30
$CHCl_3$	—	503, 617	—	< 0.01
DCM	—	610	—	0.26
MeCN	493	661	0.01	0.29
DMF	522	661	0.06	0.36
DMSO	527	663	0.04	0.34
EtOH	533	657	0.05	0.13
MeOH	544	657	0.05	0.09
H_2O	611	660	< 0.01	0.03

Synthesis of T2OH1BT and T2OH1BI

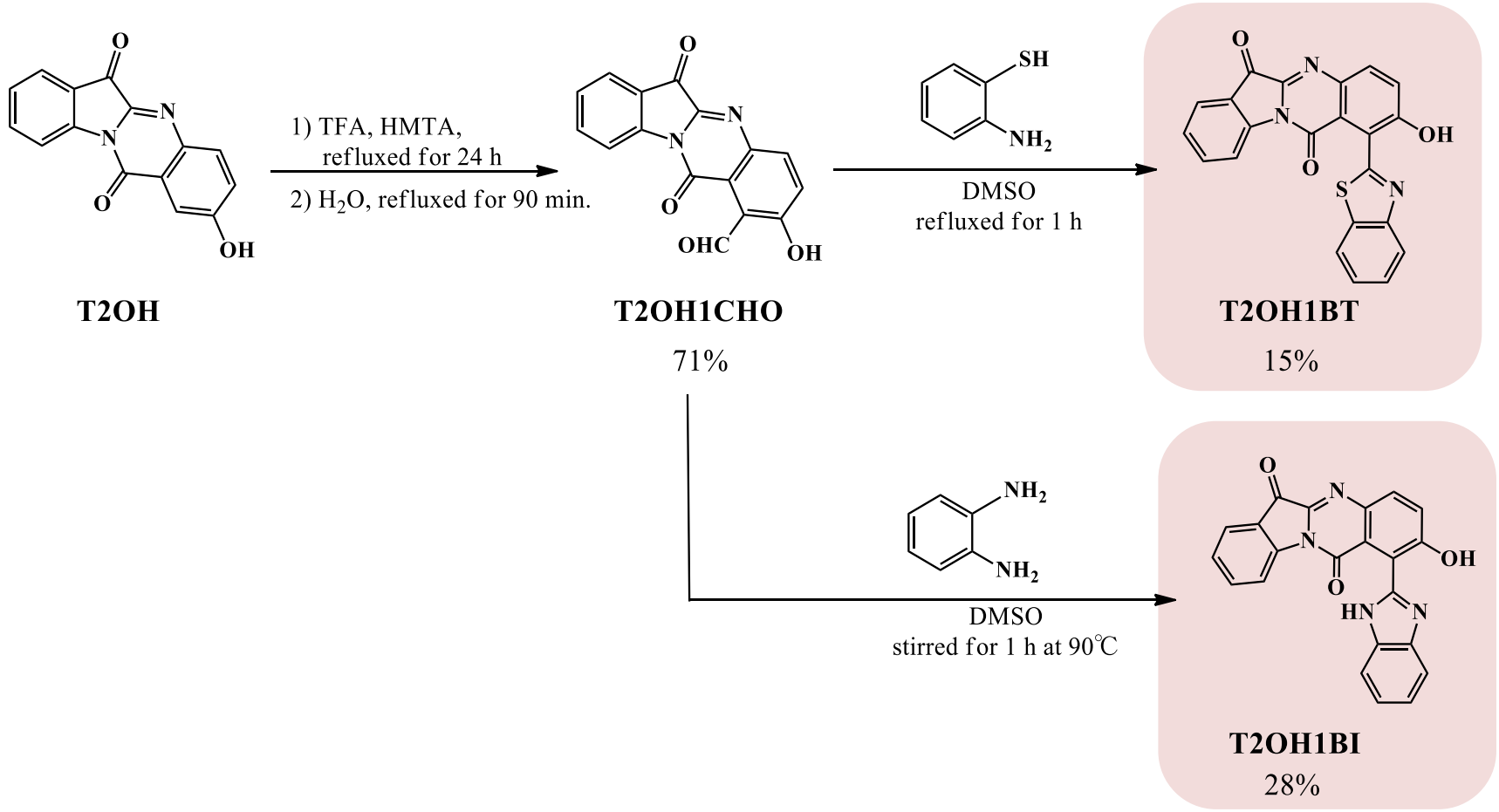

Absorption spectra of T2OH, T2OH1BT and T2OH1BI

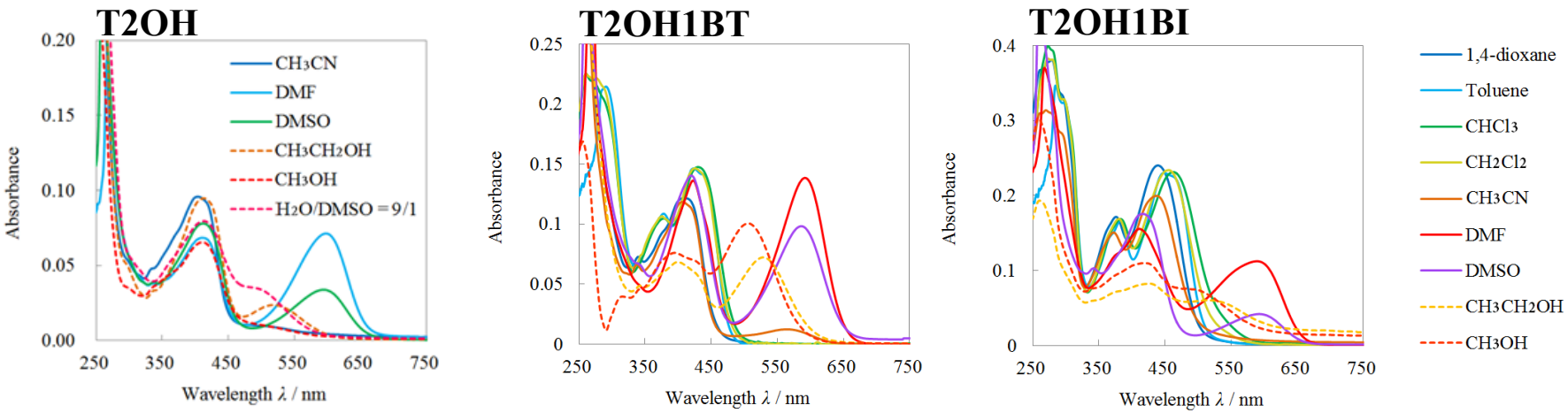

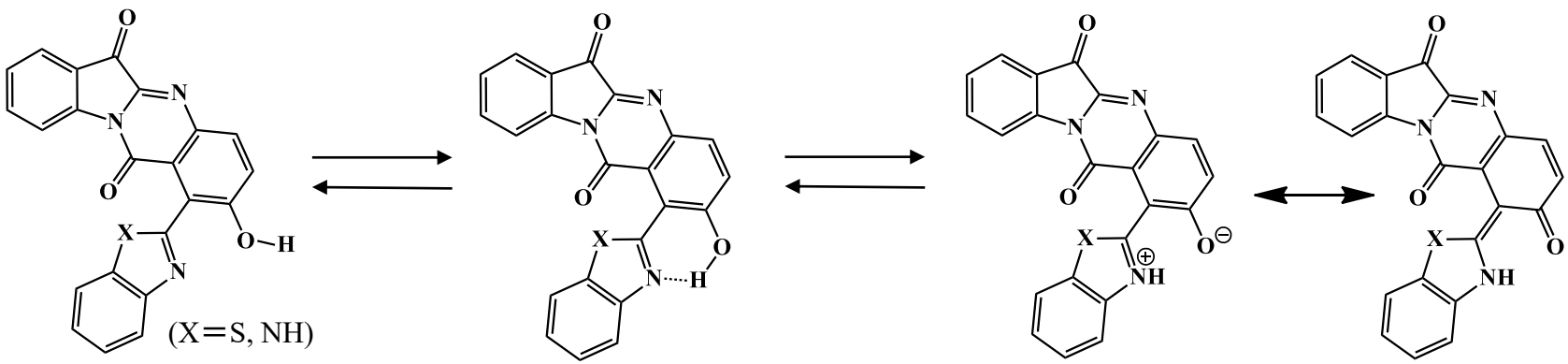

Open conformer

Closed conformer

Proton dissociation

DFT calculation results of T2OH1BT and T2OH1BI

Ground State

(a) **T2OH1BT**

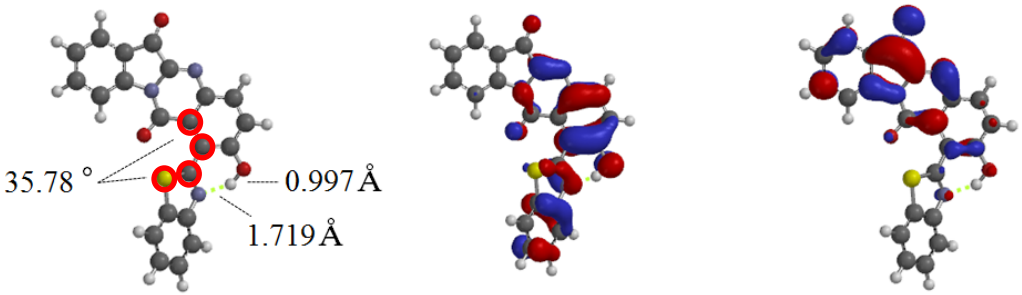

(b) **T2OH1BI**

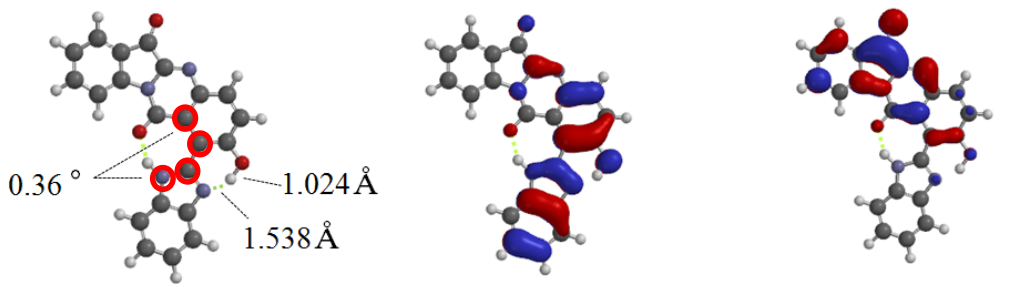

Optimized Structure HOMO LUMO

Solvents	$\lambda_{a,max}$ / nm	
	T2OH1BT	**T2OH1BI**
1,4-DOX	340, 409	376, 439
PhMe	378, 423	382, 449
$CHCl_3$	378, 430	383, 462
DCM	375, 425	380, 456
MeCN	370, 406	372, 437
DMF	422, 592	411, 590
DMSO	420, 586	416, 593
EtOH	399, 528	427, 515
MeOH	395, 506	419, 510

Optimized structure and FMO of (a) **T2OH1BT** and (b) **T2OH1BI** calculated by DFT B3LYP 6-31+G* in vacuum

Fluorescence spectra of T2OH1BT and T2OH1BI

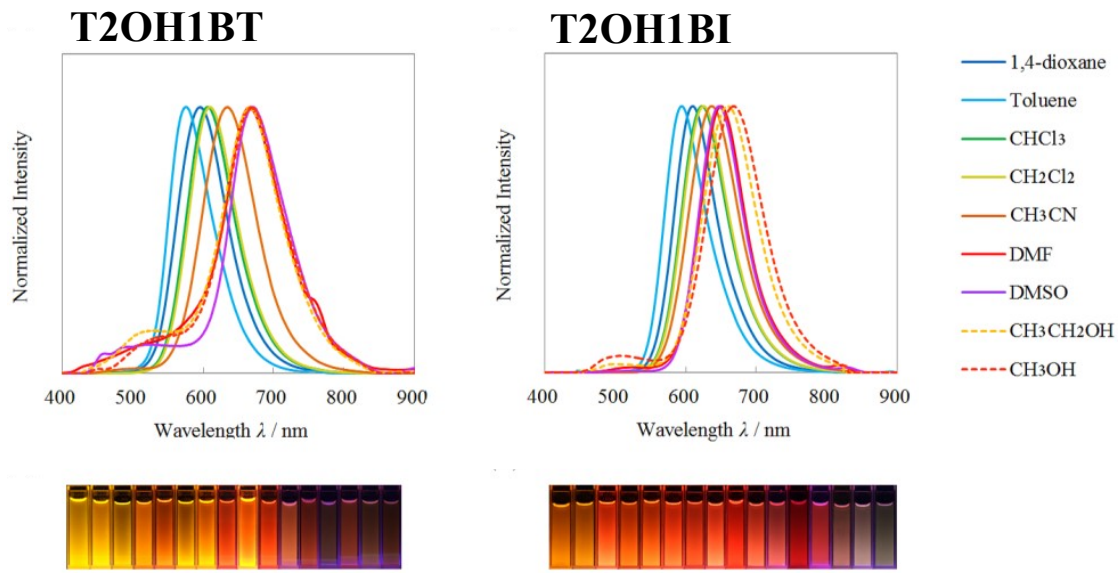

Solvents	$\lambda_{f,max}$ / nm		Φ_f	
	T2OH1BT	**T2OH1BI**	**T2OH1BT**	**T2OH1BI**
1,4-DOX	595	610	0.19	0.22
PhMe	575	599	0.38	0.49
$CHCl_3$	606	627	0.41	0.35
DCM	609	630	0.35	0.29
MeCN	634	642	0.14	0.25
DMF	667	650	0.04	0.1
DMSO	671	647	0.03	0.05
EtOH	668	659	0.02	0.03
MeOH	670	667	0.01	0.01

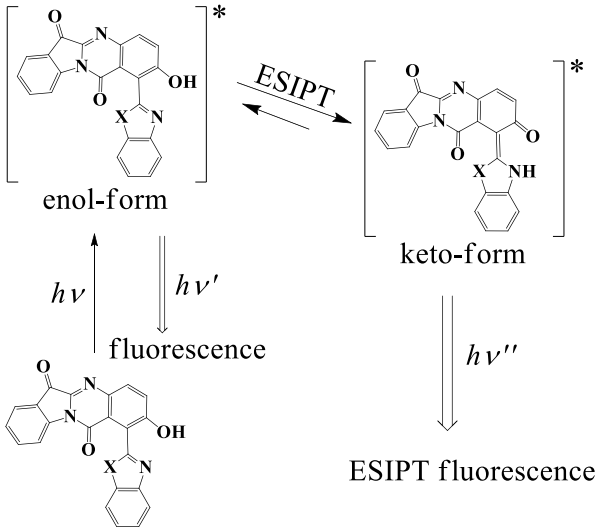

T2OH1BT (X = S)
T2OH1BI (X = N)

DFT calculation results of T2OH1BT and T2OH1BI

Excited State

(a) **T2OH1BT**

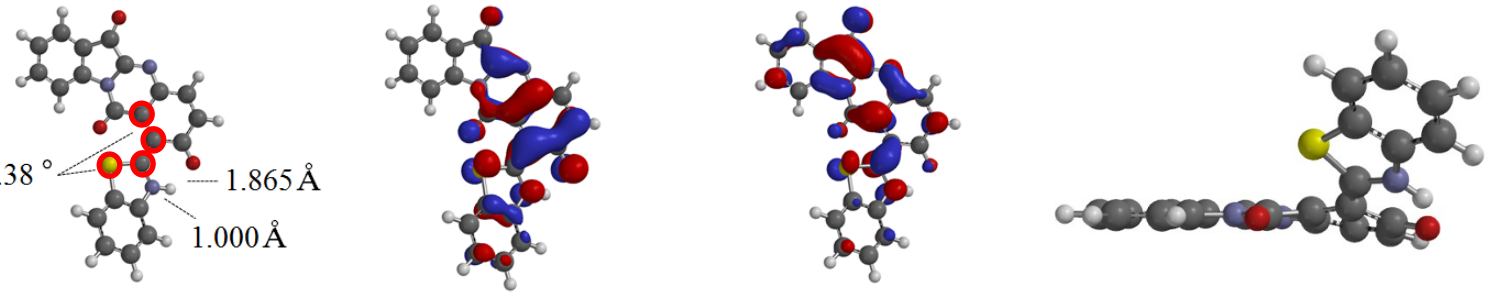

(b) **T2OH1BI**

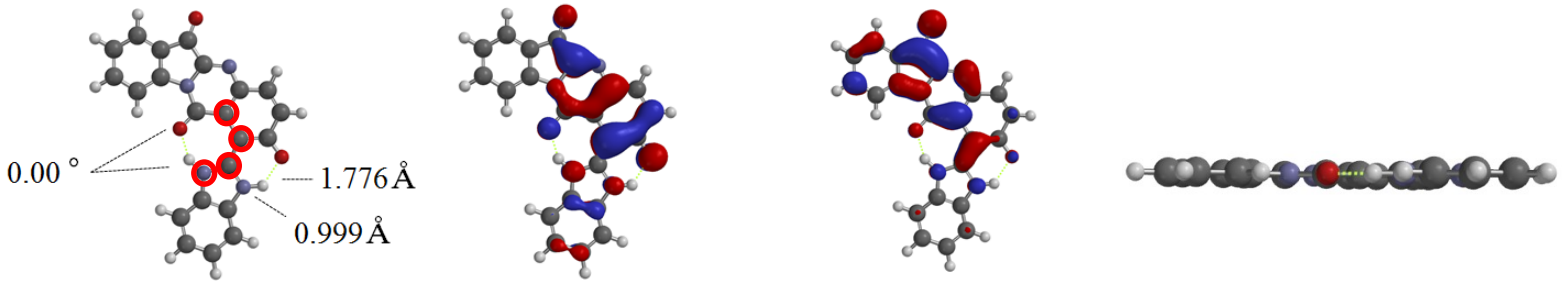

Optimized Structure HOMO LUMO

Optimized structure of (a) **T2OH1BT** and (b) **T2OH1BI** calculated by CIS 6-31G** and FMO by DFT B3LYP 6-31+G* in vacuum

Emission in the Solid State

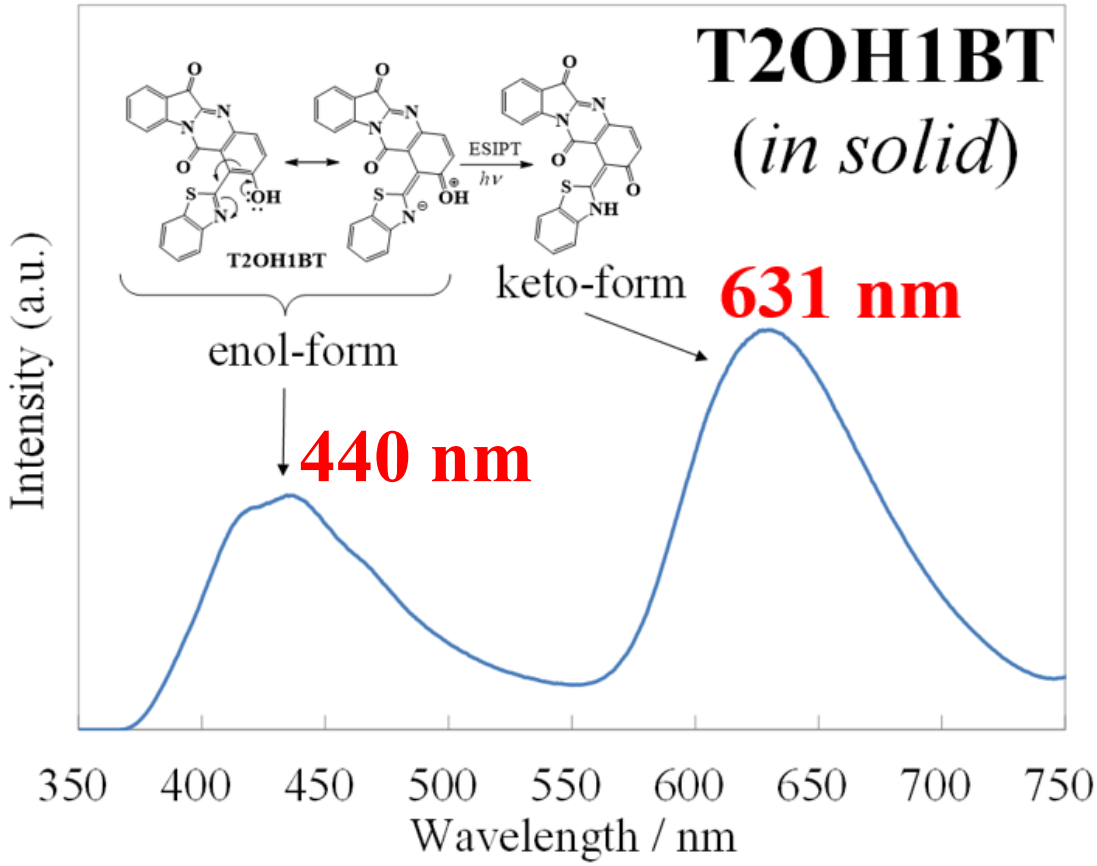

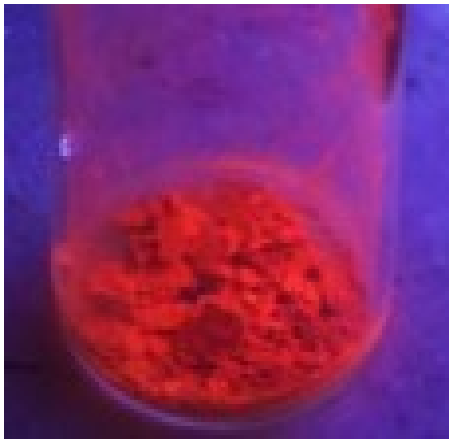

Fluorescence spectra of **T2OH1BT** in solid.

1-Benzothiazolyl-2-hydroxytryptanthrin (**T2OH1BT**) was synthesized as an excited state intramolecular proton transfer (ESIPT) fluorophore. In the solid state, the keto tautomer emission via ESIPT at 631 nm was observed, whereas the enol tautomer emission at 440 nm was observed.

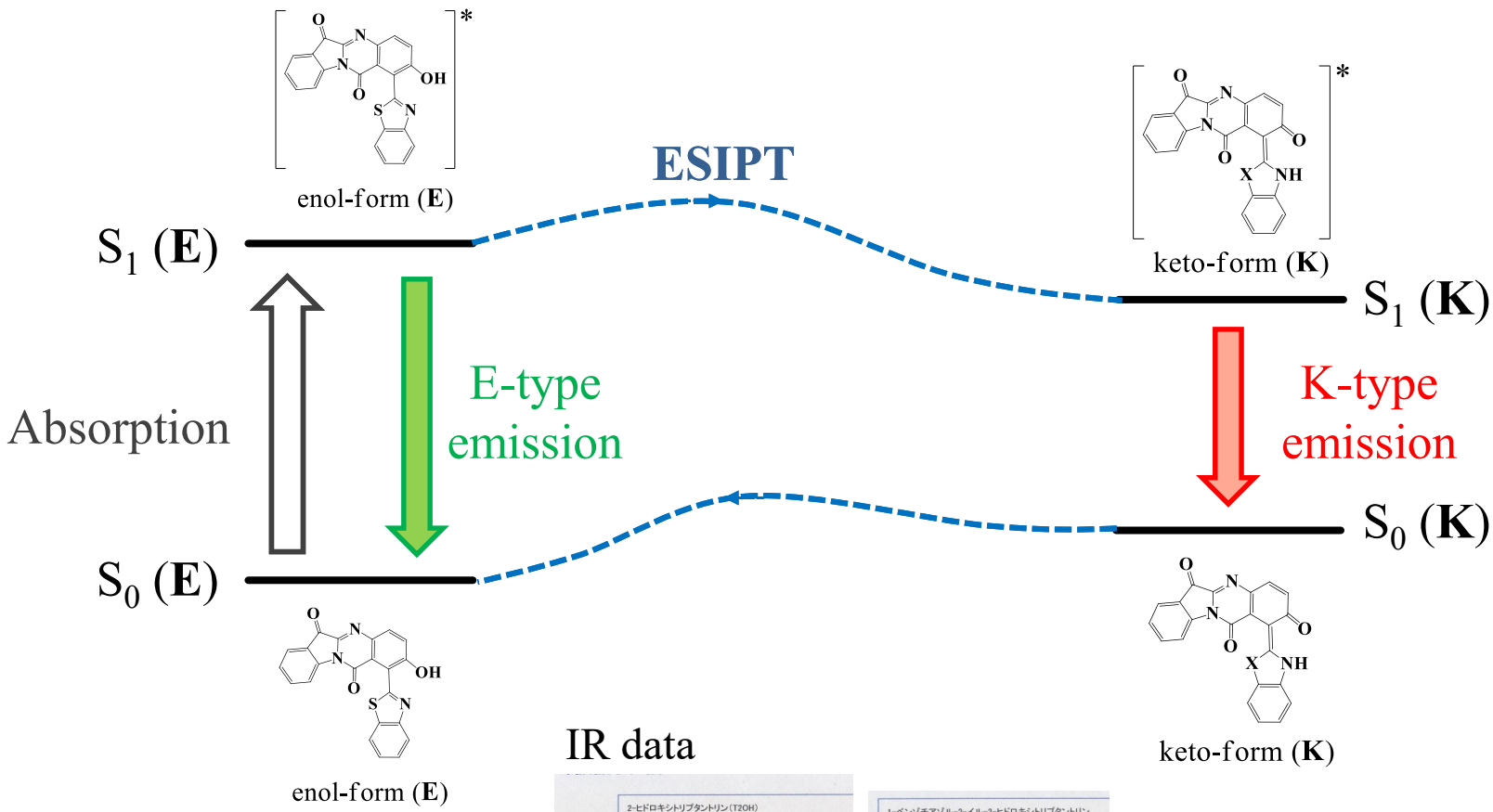
enol-form (E)
ESIPT
keto-form (K)
S1 (E)
S1 (K)
Absorption
E-type emission
K-type emission
S0 (K)
S0 (E)
enol-form (E)
keto-form (K)

IR data

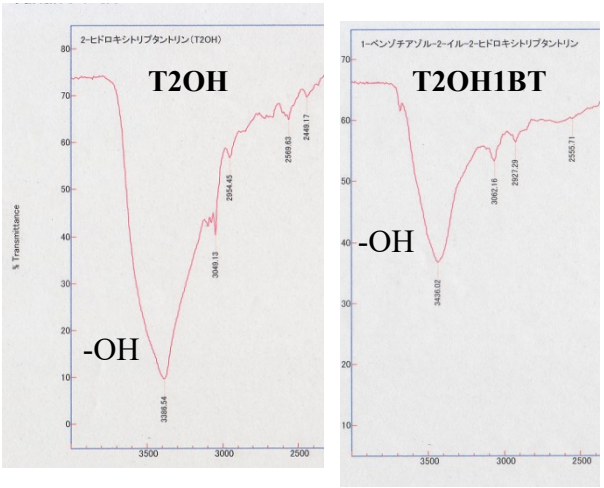
T2OH
-OH
T2OH1BT
-OH

Summary

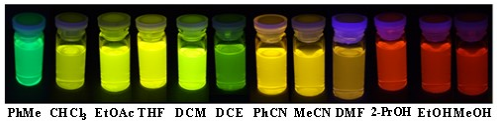

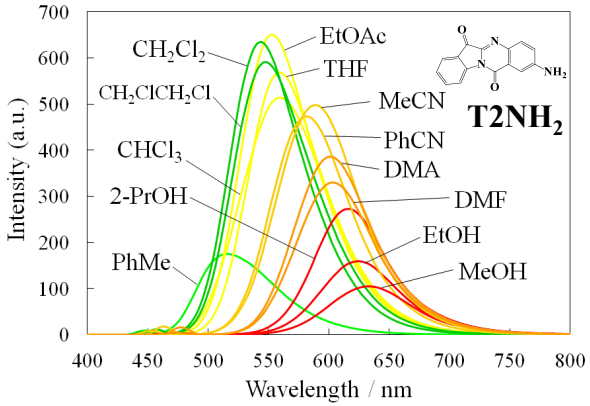

Florescence spectra in solvents of different polarity of **T2NH$_2$** [1, 2].

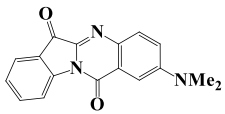

T2NMe$_2$

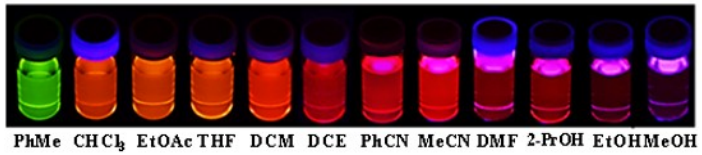

Photographs of **T2NMe$_2$** taken under 365 nm UV light in different solvents [5].

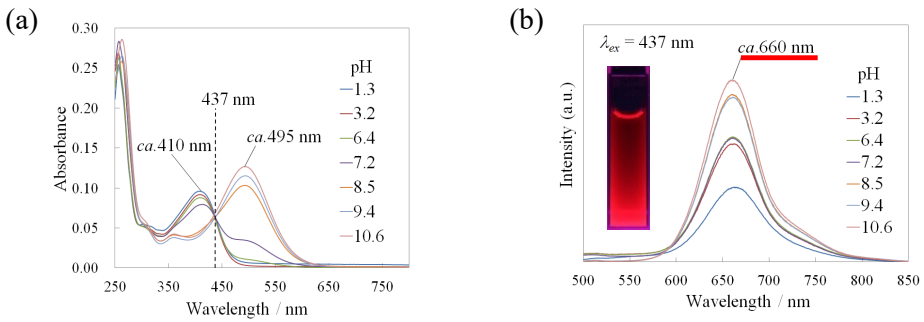

(a) UV-vis absorption and (b) fluorescence spectra of **T2OH** in a DMSO/H_2O (1/9, v/v) solution at different pH values [4].

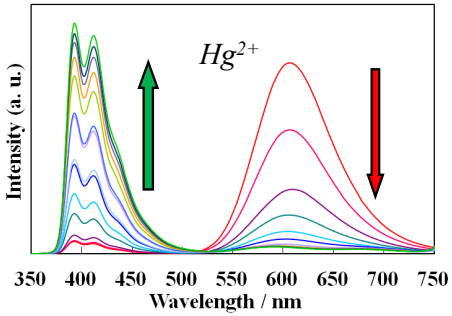

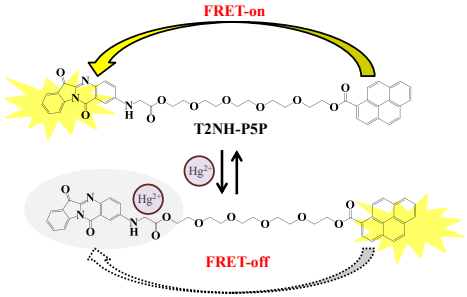

Spectral changes in the fluorescence of **T2NH-P5P** (10 mM) upon addition of $Hg(ClO_4)_2$ (0 – 1000 equiv) in acetonitrile [3].

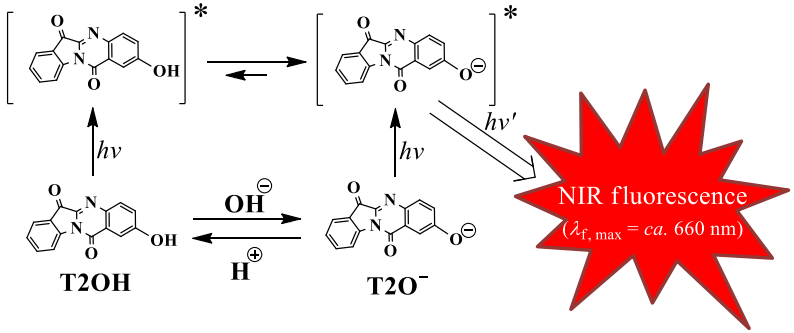

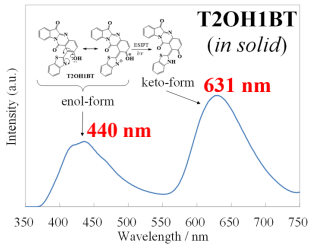

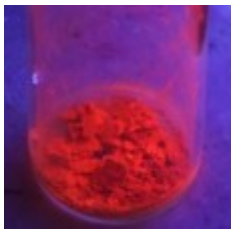

Fluorescence spectra of **T2OH1BT** in solid.

[1] J. Kawakami, Tryptanthrin Derivatives, Patent No. 5448046, Japan. [2] J. Kawakami *et al.*, *Trans. Mater. Res. Soc. Japan*, **2013**, *38*, 123-125. [3] J. Kawakami *et al.*, *Anal. Sci.*, **2014**, *30*, 949-954 (Hot Article Award). [4] J. Kawakami *et al.*, *Anal. Sci.*, **2016**, *32*, 251-253. [5] J. Kawakami *et. al.*, *Trans. Mater. Res. Soc. Japan*, **2016**, *41*, 143-146.

Acknowledgements

This work was supported by JSPS KAKENHI Grant Number 22550068, 25410137 and 16K05805 (*Apr. 1, 2010 −Mar. 31, 2019*).

Collaborators:

Hirosaki Univ.

Prof. Shunji Ito
Prof. Haruo Kitahara
Prof. Akio Nakane
Prof. Masahiko Nagaki
Assistant Prof. Kazuhiko Seya

TOHO Univ.

Prof. Yoich Habata

ChibaTech (CIT)

Assistant Prof. Mari Ikeda

Graduate Students:

Kenta Kikuchi
Masahiro Takahashi
Takuma Kadowaki
Akihiro Tsuiki
Kazunori Chiba
Yoh Kikuchi
Hiroko Kakinami
Noriyuki Matsushima
Asako Yamaya

Undergraduate students:

Arisa Soma
Hiroko Kawaguchi
Yuta Ogawa